JACS
JOURNAL OF THE AMERICAN CHEMICAL SOCIETY

Perspective

pubs.acs.org/JACS

The Supramolecular Chemistry of β-Sheets

Pin-Nan Cheng, Johnny D. Pham, and James S. Nowick*

Department of Chemistry, University of California, Irvine, Irvine, California 92697-2025, United States

ABSTRACT: Interactions among β-sheets occur widely in protein quaternary structure, protein−protein interaction, and protein aggregation and are central in Alzheimer's and other amyloid-related diseases. This Perspective looks at the structural biology of these important yet under-appreciated interactions from a supramolecular chemist's point of view. Common themes in the supramolecular interactions of β-sheets are identified and richly illustrated though examples from proteins, amyloids, and chemical model systems. β-Sheets interact through edge-to-edge hydrogen bonding to form extended layers and through face-to-face hydrophobic or van der Waals interactions to form layered sandwich-like structures. Side chains from adjacent layers can fit together through simple hydrophobic contacts or can participate in complementary interdigitation or knob−hole interactions. The layers can be aligned, offset, or rotated. The right-handed twist of β-sheets provides additional opportunities for stabilization of edge-to-edge contacts and rotated layered structures.

INTRODUCTION

The supramolecular chemistry that is central to organization and communication in living cells relies on hydrogen bonding, hydrophobic, and other noncovalent interactions between biomolecules.[1] The edge-to-edge hydrogen bonding of the A-T and C-G bases of DNA helps encode genetic information. Interactions among coiled coils, such as the leucine zippers of Fos and Jun, help regulate transcription, as do the interactions of transcription factors with DNA. Molecular recognition between antibodies and antigens is not only central to the functioning of the immune system but also serves as the basis for many biochemical assays. Unlike these well-studied interactions, the supramolecular interactions among β-sheets have not received the attention they deserve. This Perspective seeks to shed light on this important, yet under-appreciated mode of biomolecular recognition.

β-Sheet structures and interactions are ubiquitous in protein tertiary and quaternary structure, protein dimerization and oligomerization, protein−protein interaction, and peptide and protein aggregation.[2] Figure 1 illustrates some of these structures and interactions. Notably, protein aggregation through β-sheet interactions has increasingly drawn attention because it occurs in many devastating human diseases, such as AIDS,[3] cancer,[4] Alzheimer's disease,[5] prion diseases,[6] and amyloid-related diseases.[7] Understanding interactions between β-sheets not only provides insights into biomolecular recognition but also provides a prospective avenue of intervention in human diseases involving β-sheet interactions.[8]

This Perspective also aims to share the insights into β-sheet interactions that we have gained by developing chemical models of protein β-sheets that are inspired by β-sheets in proteins and peptides.[9] We have used these synthetic molecules to mimic, control, and understand the β-sheet structures and interactions that occur in the folding of β-sheets, their dimerization through exposed hydrogen bonding edges, their assembly to form quaternary structures and oligomers, and their aggregation.

β-SHEET STRUCTURES

Anatomy of β-Sheets. β-Sheets comprise extended polypeptide β-strands that are aligned laterally and hydrogen bonded and are often further stabilized by interactions between the side chains. A β-strand is a pleated linear array of amino acids whose side chains alternate above and below the polypeptide backbone (Figure 2a). The β-strands can run in either the same or opposite directions, forming either parallel or antiparallel β-sheets. The β-strands are spaced approximately 4.7−4.8 Å apart and are approximately 3.3−3.5 Å per residue in length. Parallel β-sheets form a network of hydrogen-bonded 12-membered rings (Figure 2b), while antiparallel β-sheets form a network of alternating hydrogen-bonded 10- and 14-membered rings (Figure 2c). The 10- and 14-membered rings of antiparallel β-sheets are respectively known as the hydrogen-bonded (HB) and non-hydrogen-bonded (NHB) pairs, because the amino acids in the 10-membered rings are hydrogen bonded to each other, while those in the 14-membered rings are not. The side chains of the alternate amino acids in the β-strands make up the "top" and "bottom" faces of the β-sheet, which sit above and below the hydrogen-bonded backbones (Figure 2d).

Interstrand interactions among the amino acid side chains are important in β-sheet structure and stability. Amino acids other than glycine and alanine contain β-substitutents that can interact in antiparallel and parallel β-sheets. In the NHB pairs of antiparallel β-sheets, the side chains can gear and clash to a greater extent than those in the HB pairs (Figure 2f) or in parallel β-sheets (Figure 2e). The side-chain pairing preferences of amino acids in β-sheets have been studied both experimentally and statistically,[10] and our laboratory has coauthored a database of intermolecular amino acid pairing preferences in β-sheets.[11]

Twist of β-Sheets. β-Sheets in proteins are generally not flat, like the idealized models in Figure 2, but rather are twisted in a right-handed fashion.[12] The β-sheets of the transthyretin monomer illustrate this twist (Figure 3a). One may envision this twist by holding a piece of paper horizontally (like

Received: September 5, 2012
Published: April 2, 2013

   dx.doi.org/10.1021/ja3088407 | J. Am. Chem. Soc. 2013, 135, 5477−5492

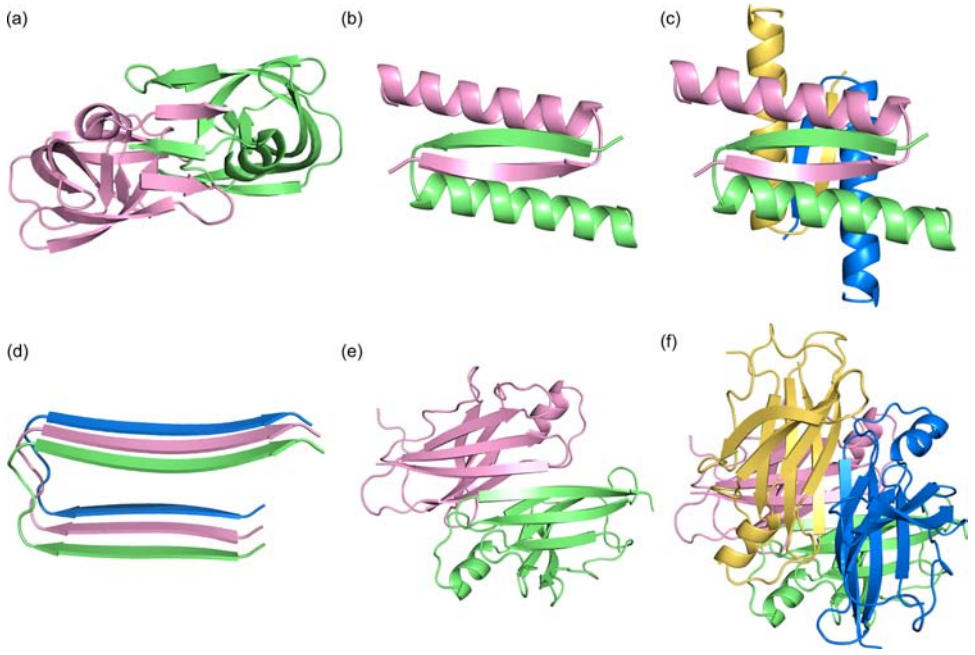

Figure 1. Representative structures and interactions of β-sheets. (a) Homodimer of HIV protease (PDB: 3HVP). (b) Homodimer of the p53 tetramerization domain (PDB: 1C26). (c) Homotetramer of the p53 tetramerization domain. (d) NMR-based model of $A\beta_{1-42}$ fibril (PDB: 2BEG). (e) Homodimer of transthyretin (PDB: 1TTR). (f) Homotetramer of transthyretin.

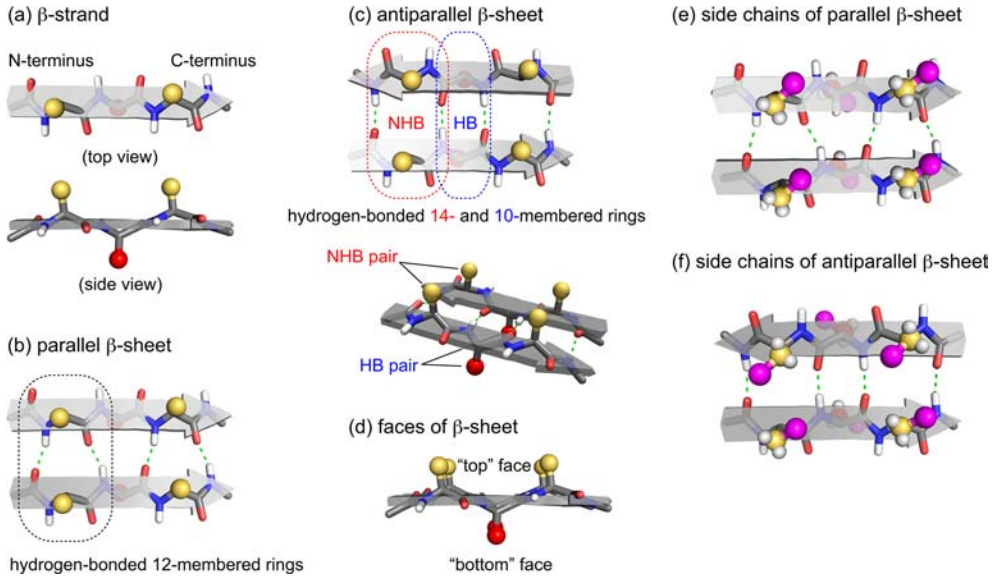

Figure 2. Anatomy of β-sheets. (a) β-Strand. (b) Parallel β-sheet. (c) Antiparallel β-sheet. (d) Faces of a β-sheet. (e) Common side chain orientation of a parallel β-sheet. (f) Common side chain orientation of an antiparallel β-sheet.

horizontal peptide β-strands) and pulling the upper right-hand and lower left-hand corners toward each other, above the plane of the page, while simultaneously pushing the upper left-hand and lower right-hand corners toward each other below the plane of the page (Figure 3b).

***β*-Sandwich.** β-Sheets in proteins do not typically occur as isolated structures but rather pack through hydrophobic interactions with α-helices or other β-sheets to create compact globular tertiary (intramolecular) or quaternary (intermolecular) structures. β-Sandwiches form when two β-sheets pack together through hydrophobic face-to-face interactions.[1] The β-sheets are typically about 10 Å apart. Often the β-sheets comprising this sandwich-like structure present more hydrophilic faces to water. β-Sandwiches are abundant in protein tertiary domains, and assembly among β-sandwiches often provides unique quaternary protein structures with specific functions. Figure 3a illustrates the β-sandwich structure of transthyretin, which forms quaternary structures that transport thyroxine and retinol.[13]

Two β-sandwiches can further assemble through face-to-face interactions to form four-layered structures. The immunoglobulin G (IgG) light and heavy chains assemble to form functional antibodies through face-to-face quaternary interactions between the β-sandwiches of these two components. The resulting four-layered β-sandwich acts as a scaffold to display six loops as a specific binding site for antigens. Figure 4

dx.doi.org/10.1021/ja3088407 | J. Am. Chem. Soc. 2013, 135, 5477−5492

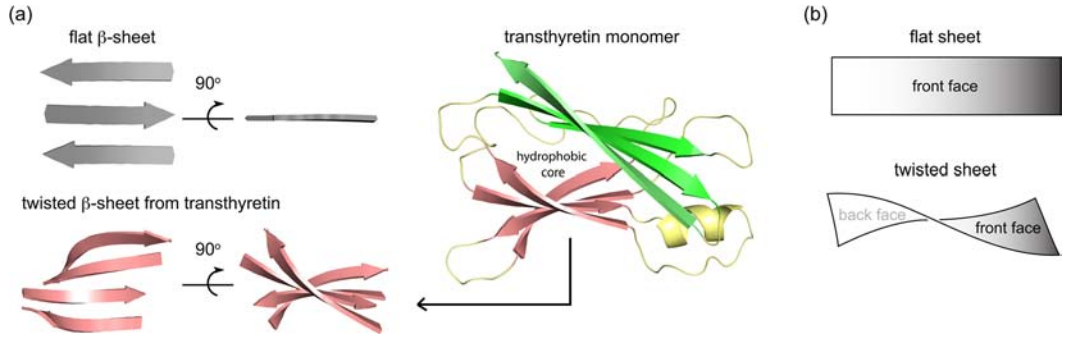

Figure 3. Twist of β-sheets. (a) Cartoons of a flat β-sheet and the twisted β-sheets of transthyretin (PDB: 1TTR). (b) Representation of sheets of paper with flat and twisted surfaces.

illustrates these structures and interactions in immunoglobulin G2a (IgG2a).[14]

***β*-Barrel.** β-Sheets can also pack to form closed structures without exposed hydrogen-bonding edges, in which the β-strands resemble staves in a barrel. Small β-barrel structures can resemble a β-sandwich in which the edges of the two layers have hydrogen bonded together; larger β-barrels generally form a cavity that can accommodate additional matter within. Figure 5 illustrates a variety of β-barrels.

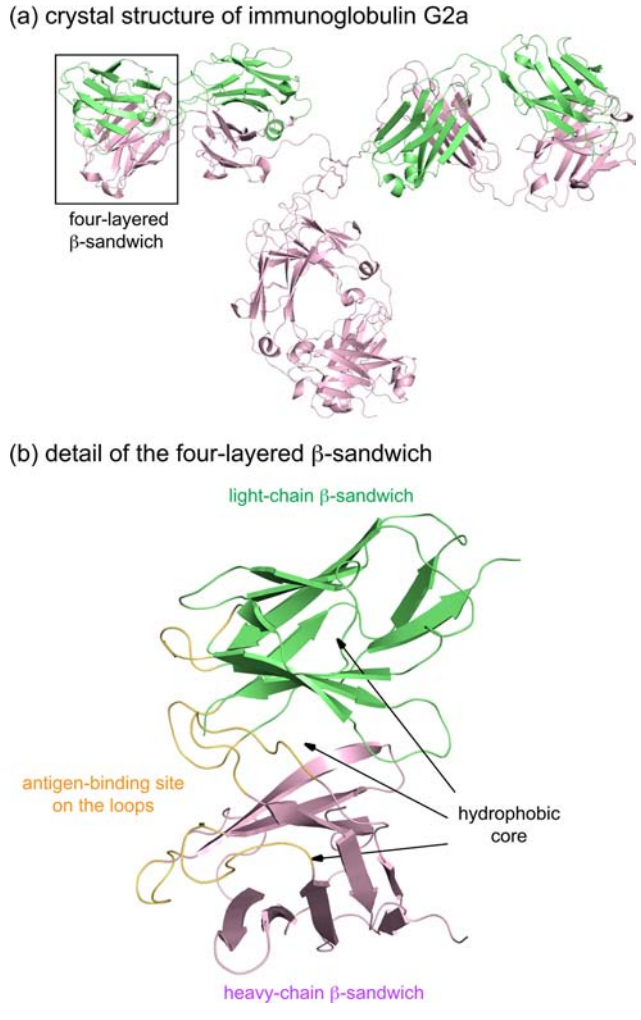

Figure 4. β-Sandwich structures. (a) Immunoglobulin G2a (PDB: 1IGT). (b) Detail illustrating the specific antigen-binding site of IgG2a, the hydrophobic cores of the light- and heavy-chain β-sandwiches, and the hydrophobic core between two β-sandwiches.

β-Barrels occur widely in enzymes, protein transporters, membrane pores, and binding proteins.[1] The human plasma retinol-binding protein (RBP), for example, contains an eight-stranded β-barrel with a hydrophobic cavity that binds retinol and facilitates its transport (Figure 5a,b).[15] The membrane protein FhaC is an essential component of the protein transporter machinery for gram-negative bacteria and eukaryotic organelles.[16] It contains a 16-stranded β-barrel with a hydrophilic cavity containing 17 charged residues. When FhaC is inactive, the cavity of the β-barrel is plugged by an α helix that displays complementary charged residues (Figure 5c,d). When FhaC is active and helps translocate proteins across the membrane, the cavity is unplugged so that proteins can translocate through the cavity.

β-Barrels may also play an important role in the elusive structures of small amyloid oligomers, which are generally thought to be the key neurotoxic species in Alzheimer's and other neurodegenerative diseases.[17] Thus, an oligomer of an amyloidogenic peptide fragment from αB crystallin was recently found to form a six-stranded β-barrel containing three pairs of antiparallel β-sheets and a filled interior (Figure 5e).

***β*-Helix.** A β-sheet structure that is less common in globular proteins—the β-helix—sets the stage for the structures of amyloid fibrils, the visible hallmark of Alzheimer's and many other diseases involving protein aggregation. β-Helices are helical structures composed of alternating β-strands and loops that run nearly orthogonal to the helical axis. The β-strands hydrogen bond together to form parallel β-sheets, which are often arranged in a triad about the helical axis. The β-sheets may collapse on each other forming sandwich-like structures or may form a triangular cavity, like a β-barrel. Figure 6 illustrates three representative β-helix structures.

The β-helix was first discovered in the bacterial protein pectate lyase C in 1993.[18] The β-helix of pectate lyase C consists of a single polypeptide chain that coils into three parallel β-sheets separated by loops (Figure 6a). The β-sheets form a collapsed structure in which two of the three sheets make a sandwich-like structure, and the third, in conjunction with additional loops, spans the layers of the sandwich. β-Helices can also form through the assembly of multiple polypeptide chains. The β-helix of the $(gp27\text{-}gp5^{*}\text{-}gp5C)_3$ complex of the cell-puncturing device of bacteriophage T4 is a triple helix comprising three separate polypeptide chains wrapped about the helical axis to give a triangular cavity (Figure 6b).[19] β-Helices are integral to the aggregation of the fungal HET-s prion-forming protein that aggregates to form amyloid

dx.doi.org/10.1021/ja3088407 | J. Am. Chem. Soc. 2013, 135, 5477−5492

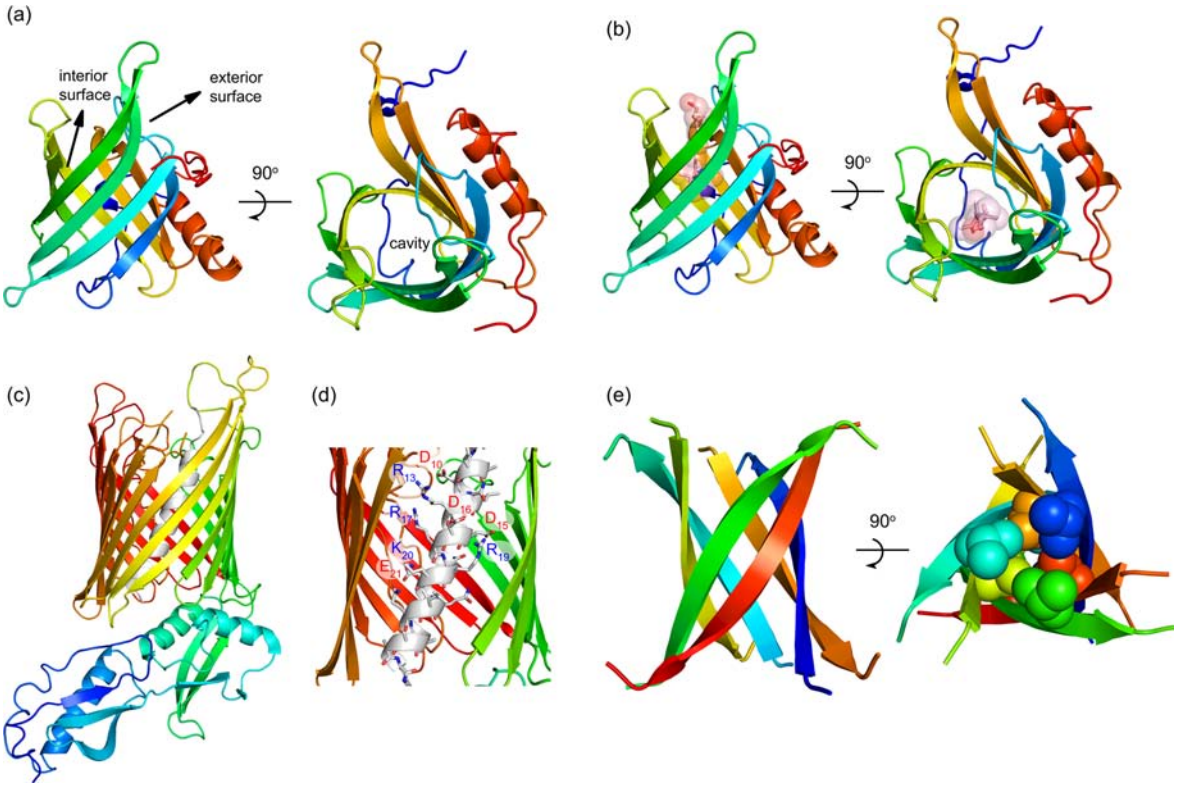

Figure 5. β-Barrel structures. (a) Eight-stranded β-barrel of human plasma retinol-binding protein (PDB: 1BRP). (b) Complex of human plasma retinol-binding protein and retinol. (c) The 16-stranded β-barrel of the membrane protein FhaC (PDB: 2QDZ). (d) Cutaway view of the 16-stranded β-barrel of FhaC. (e) Six-stranded β-barrel formed by peptide fragment KVKVLGDVIEV (K11V) derived from protein αB crystallin (PDB: 3SGO).

fibrils.[20] A fragment comprising residues 218−289 of HET-s has been shown to form a stack of β-helices running along the fibril axis (Figure 6c).

Higher-Order Supramolecular Structures of β-Sheets. β-Sheets have a propensity to form four-layered sandwich structures.[21] β-Sandwiches and β-helices with hydrophobic exterior surfaces can further self-assemble through hydrophobic interactions into higher-order structures containing four-layered sandwiches. The C_2 symmetric form of amyloid β-peptide ($A\beta_{1-40}$) fibrils associated with Alzheimer's disease consists of a four-layered β-sandwich similar to that of IgG (above).[22] The fibrils comprise two β-sandwiches formed by two separate networks of $A\beta_{1-40}$ tightly laminated through hydrophobic interactions to form a C_2 symmetric four-layered β-sandwich structure (Figure 7a, green and pink structures). $A\beta_{1-40}$ fibrils also form as a C_3 symmetric polymorph, which shares structural features with the C_2 form but lacks the tight lamination.[23] In this polymorph, two β-sandwiches tilt to form a more loosely laminated four-layered structure that can accommodate the third β-sandwich (Figure 7b). A similar sort of C_3 symmetric structure occurs in the P22 tail-spike protein, which consists of a supramolecular assembly of three β-helices (Figure 7c).[24]

■ β-SHEET INTERACTIONS THROUGH EDGE-TO-EDGE HYDROGEN BONDING

Dimerization of folded proteins through the exposed hydrogen-bonding edges of β-sheets is a fundamental type of protein−protein interaction that is common in protein structure.[2a] The topology of a folded protein with an exposed β-sheet hydrogen-bonding edge favors intermolecular hydrogen bonding to form a C_2 symmetric antiparallel β-sheet dimerization interface. Hydrophobic interactions between the hydrophobic residues of the interface and the hydrophobic interior of the protein typically stabilize the dimerization interface. The resulting quaternary structures can involve multiply stranded β-sheets, individual β-strands, or the interdigitation of β-strands and are often necessary for the biological function of the protein.

β-Sheet Dimerization of Multiply Stranded β-Sheets. The protein ParB forms a homodimer that helps partition DNA at cell division.[25] ParB dimerizes by forming an antiparallel β-sheet dimerization interface in which the exposed edges of two three-stranded β-sheets hydrogen bond to form six hydrogen bonds (Figure 8a). The interface is further stabilized through hydrophobic contact between residues F_{300}, Y_{302}, and F_{304} of the interface and the hydrophobic surface created by the α-helices of the protein (Figure 8b).

Transthyretin helps transport thyroid hormones and retinol and functions as a homotetramer comprising a dimer of β-sheet dimers (Figure 1f).[26] Transthyretin dimerizes by forming an antiparallel β-sheet dimerization interface between two three-stranded β-sheets (Figure 1e). Two of the dimers further self-assemble into a homotetramer through hydrophobic contact (Figure 1f).

β-Sheet Dimerization of Single β-Strands. The *met* repressor protein helps regulate the biosynthesis of methionine and functions as a homodimer. The *met* repressor protein dimerizes by forming an antiparallel β-sheet dimerization interface in which the two single β-strands hydrogen bond to form eight hydrogen bonds (Figure 9a).[27] The interface is further stabilized through hydrophobic contact between residues I_{24}, V_{26}, and I_{28} of the interface and the hydrophobic surface created by the α-helices of the protein (Figure 9b).

dx.doi.org/10.1021/ja3088407 | J. Am. Chem. Soc. 2013, 135, 5477−5492

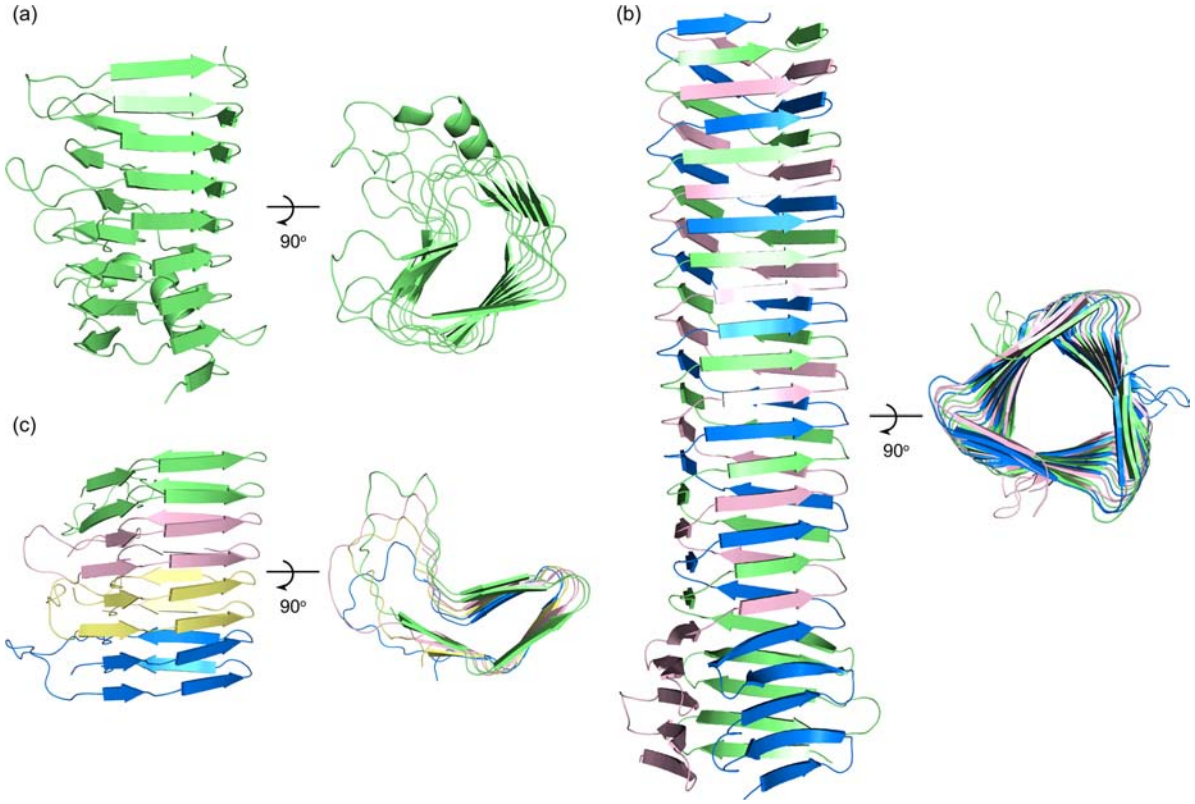

Figure 6. β-Helix structures. (a) β-Helix formed by pectate lyase C (PDB: 2PEC). (b) Trimeric β-helix of the $(gp27\text{-}gp5^{*}\text{-}gp5C)_3$ complex of the cell-puncturing device of bacteriophage T4 (PDB: 1K28). (c) Stack of β-helices formed by residues 218−289 of HET-s (PDB: 2RNM). Colors in these figures represent different polypeptide chains. Extraneous residues are omitted for clarity.

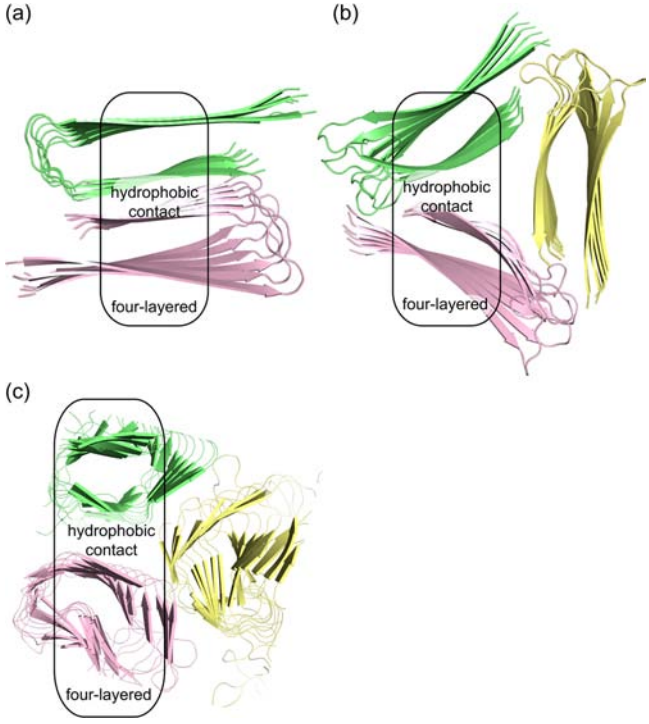

Figure 7. Four-layered β-sandwich structures. (a) C_2 symmetric form of $A\beta_{1-40}$ fibrils. (b) C_3 symmetric form of $A\beta_{1-40}$ fibrils. (c) Triangular superstructure with C_3 symmetry formed by the P22 tail-spike protein (PDB: 1TSP). Extraneous residues are omitted for clarity.

The tumor suppressor protein p53 is a 393-residue transcription factor that functions as a homotetramer and helps prevent the development of cancer.[28] The homotetramer may be thought of as a dimer of dimers, in which interactions between individual β-strands mediate dimer formation. Residues 325−356 make up the tetramerization domain. The p53 tetramerization domain dimerizes by packing two α-helices in an antiparallel fashion and by forming an antiparallel β-sheet dimerization interface (Figure 1b).[29] In this interface, two single β-strands hydrogen bond to form eight hydrogen bonds (Figure 10a). The interface is further stabilized through hydrophobic contact between residues F_{328}, L_{330}, and I_{332} of the interface and the hydrophobic surface created by the α-helices (Figure 10b). The homotetramer assembles through hydrophobic contact between the four pairs of residues L_{344} and L_{348} of the α-helices (Figure 10b).

β-Sheet Dimerization through Interdigitation of β-Strands. HIV-1 protease is an important drug target that is essential for reproduction of the AIDS virus and functions as a homodimer (Figure 1a).[30] It dimerizes by forming an antiparallel β-sheet dimerization interface in which two β-strands of each protein interdigitate to form a four-stranded antiparallel β-sheet (Figure 11a). The four-stranded β-sheet interface is further stabilized not only by hydrophobic contact between residues I_3, L_{97}, and F_{99} of the interface and the hydrophobic surface created by the protein (Figure 11b) but also by additional hydrogen bonding between side chains of Q_2 and N_{98} and between the N- and C-termini (Figure 11a).

dx.doi.org/10.1021/ja3088407 | J. Am. Chem. Soc. 2013, 135, 5477−5492

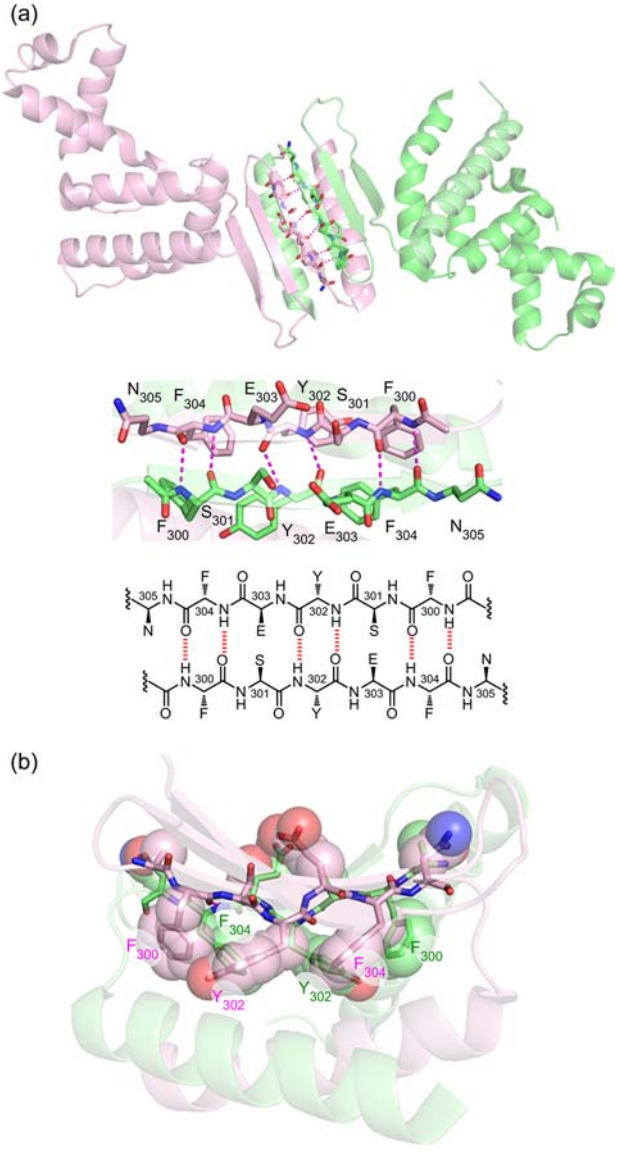

Figure 8. β-Sheet dimerization interface between two multiply stranded β-sheets of protein ParB. (a) Homodimer of ParB and detail of the antiparallel β-sheet dimerization interface of ParB homodimer (PDB: 1ZX4). (b). Hydrophobic contact between residues F_{300}, Y_{302}, and F_{304} of the dimerization interface and the hydrophobic surface created by the α-helices of the protein.

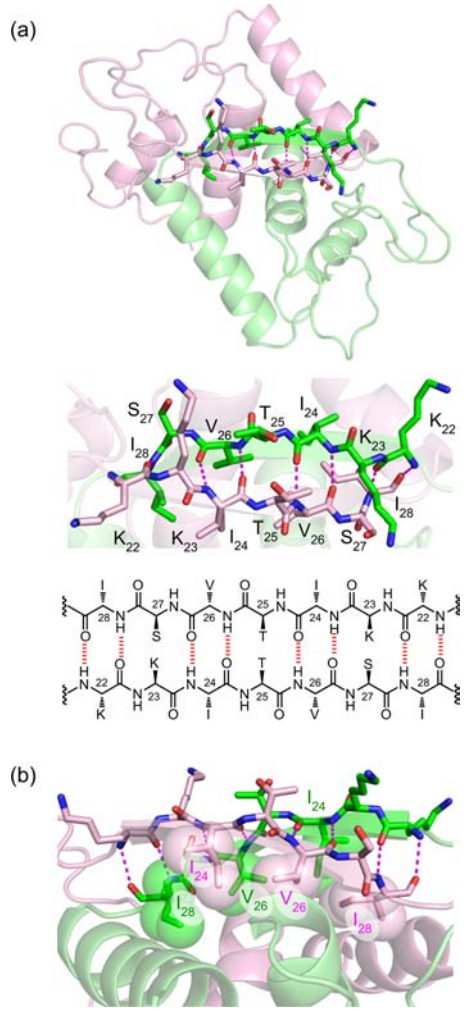

Figure 9. β-Sheet dimerization of single β-strands of the *met* repressor protein. (a) Homodimer of the *met* repressor and detail of the antiparallel β-sheet dimerization interface of the *met* homodimer (PDB: 1CMB). (b) Hydrophobic contact between residues I_{24}, V_{26}, and I_{28} of the antiparallel β-sheet dimerization interface and the hydrophobic surface created by the α-helices of the protein.

■ β-SHEET INTERACTIONS THROUGH FACE-TO-FACE INTERACTIONS

Assembly through face-to-face interactions between β-sheets is another fundamental type of protein−protein interaction that is common in protein and amyloid structure. Face-to-face interactions among β-sheets occur not only in protein tertiary and quaternary structures, such as β-sandwiches and β-helices but also in higher-order superstructures, such as the four-layered sandwich structures of Aβ_{1-40} amyloid fibrils and IgG as described above. These face-to-face interactions typically involve hydrophobic surfaces with good shape complementarity that are held together through van der Waals interactions and the hydrophobic effect.

Face-to-Face Interactions of Layered β-Sheets. Face-to-face interactions between layered β-sheets typically involve hydrophobic contact, interdigitation, or knob−hole interactions between opposing residues (Figure 12). Hydrophobic contact occurs in aligned or offset structures and typically features a large contact area created by large nonpolar side chains (Figure 12a). Contact can occur either in an aligned fashion, in which residue *j* primarily contacts its intersheet neighbor *i*, or in an offset fashion, in which residue *j* primarily contacts its intersheet neighbors *i* and *i* + 2. Face-to-face interaction through hydrophobic contact generally favors the large, branched, nonpolar side chains of valine, leucine, isoleucine, and phenylalanine, because they can provide large hydrophobic areas for intimate contact and thus maximize van der Waals interaction and the hydrophobic effect. Although large nonpolar residues are favored, some polar residues, such as tyrosine, tryptophan, serine, and threonine, can also participate.

Interdigitation occurs in offset structures and features a zipper-like packing in which side chains of the two sheets interdigitate tightly. Figure 12b illustrates this interaction in which residue *j* is embedded between intersheet neighbors *i* and *i* + 2. Interdigitation often involves uncharged unbranched residues, such as alanine, asparagine, and glutamine. These tight

dx.doi.org/10.1021/ja3088407 | J. Am. Chem. Soc. 2013, 135, 5477−5492

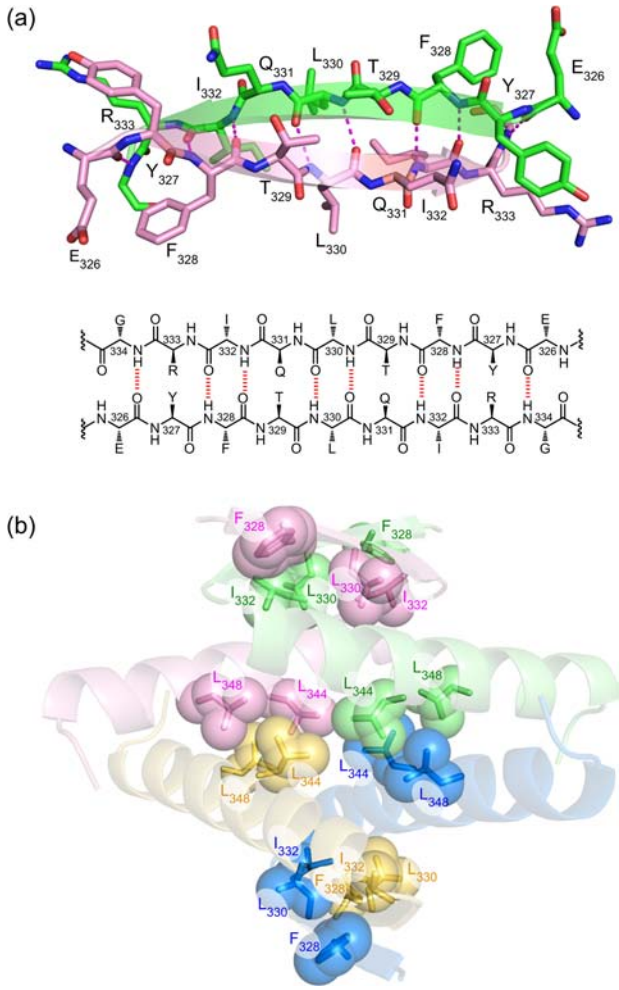

Figure 10. β-Sheet dimerization of single β-strands of the p53 tetramerization domain and further assembly to form the tetramer. (a) Antiparallel β-sheet dimerization interface of the p53 tetramerization domain homodimer (PDB: 1C26). (b) Hydrophobic contact between residues F_{328}, L_{330}, and I_{332} and the hydrophobic surface created by the α-helices; hydrophobic contact between the four pairs of residues L_{344} and L_{348} of the α-helices in the tetramer.

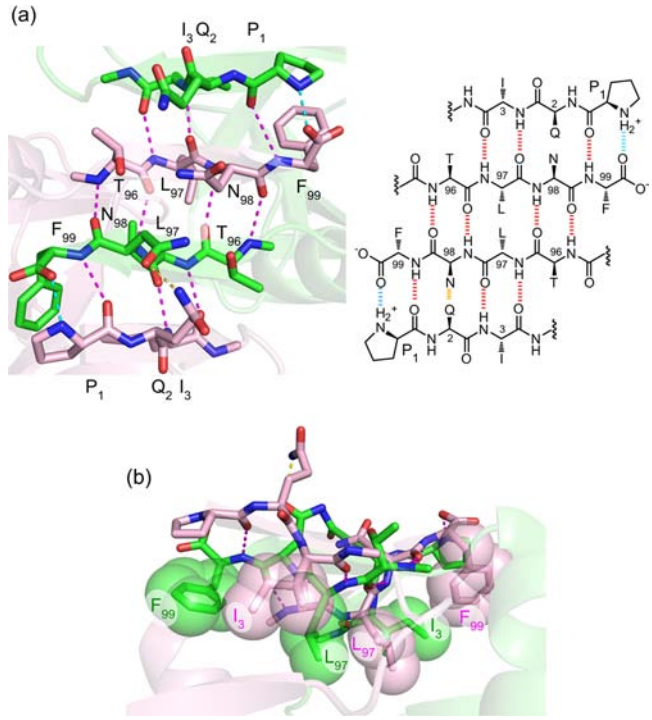

Figure 11. β-Sheet dimerization interface through interdigitation of β-strands of HIV-1 protease. (a) Four-stranded antiparallel β-sheet dimerization interface of the HIV protease homodimer (PDB: 3HVP). The side-chain hydrogen bond between Q_2 and N_{98} is shown in yellow and the salt bridges between the N- and C-termini are shown in cyan. (b) Hydrophobic contact between residues I_3, L_{97}, and F_{99} of the dimerization interface and the hydrophobic surface created by the protein.

interresidue contacts involve hydrophobic interactions and may involve hydrogen bonding with the exclusion of water.

Knob–hole interaction occurs in aligned structures and features a knob-into-hole-like packing in which a large residue serving as a knob is tightly buried in a hole created by a small residue, such as glycine or alanine. Figure 12c illustrates knob–hole interaction in which residue j is aligned with intersheet neighbor i and primarily contacts intersheet neighbors $i - 2$ and $i + 2$. Unlike interdigitation, residue j is not embedded between residues i and $i + 2$. Knob–hole interaction in β-sheets is reminiscent of the knob-into-hole packing in α-helix coiled coils.[31] Although both van der Waals interaction and the hydrophobic effect are important in knob–hole interaction, the steric complementarity of knobs and holes between layered β-sheet structures is critical to this interaction.

Orientations of Layered β-Sheets. Layered β-sheets can adopt different orientations to achieve optimal face-to-face packing. The β-sheets in the adjacent layers can be aligned, offset, or rotated, as illustrated in Figure 13. In an aligned orientation, the β-strands of the two layers overlap, so that the side chains of a β-strand in one layer interact primarily with

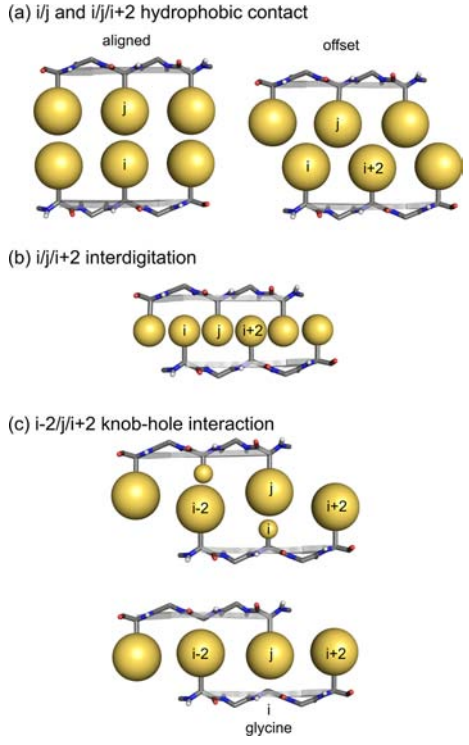

Figure 12. Face-to-face interactions of β-sheets. (a) The i/j and $i/j/i + 2$ hydrophobic contact. (b) The $i/j/i + 2$ interdigitation. (c) The $i - 2/j/i + 2$ knob–hole interaction.

dx.doi.org/10.1021/ja3088407 | J. Am. Chem. Soc. 2013, 135, 5477–5492

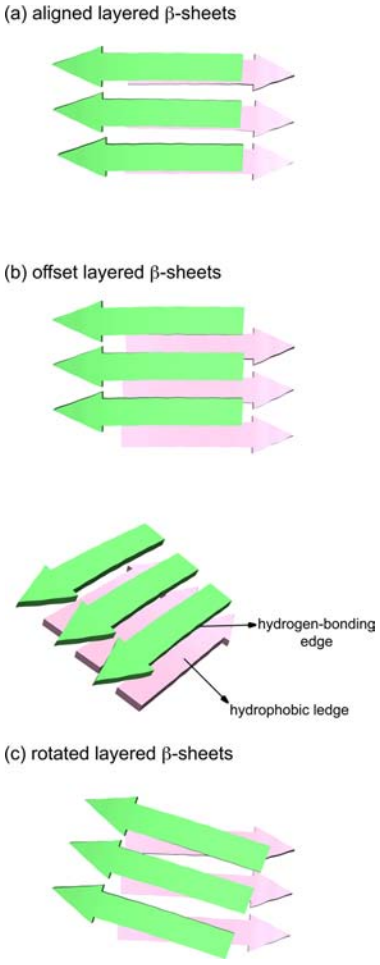

Figure 13. Orientation of layered β-sheets. (a) Aligned, (b) offset, and (c) rotated layered β-sheets.

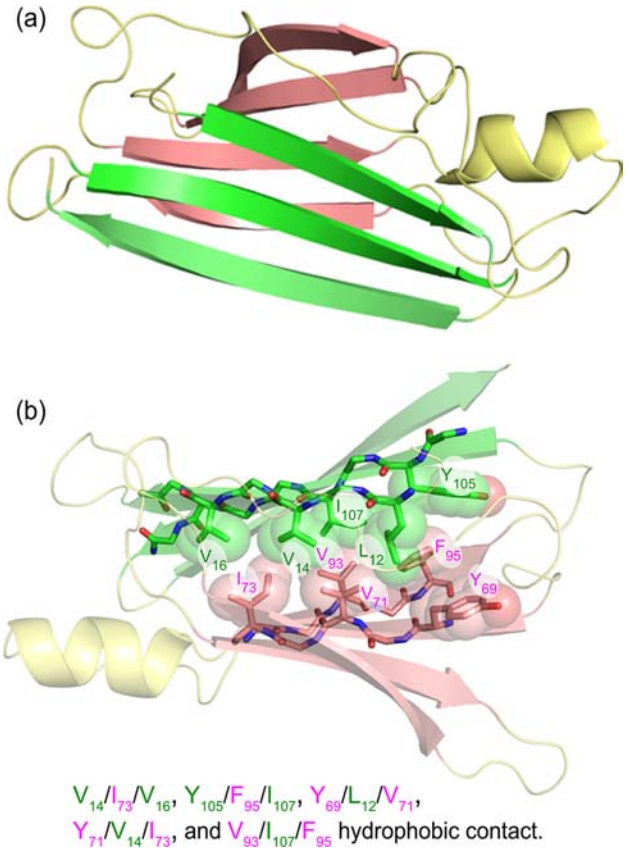

Figure 14. Orientation and face-to-face interactions in the layered β-sheets of the TTR β-sandwich (PDB: 1TTR). (a) Rotated layered β-sheets of the TTR β-sandwich. (b) The $i/j/i + 2$ hydrophobic contacts in the TTR β-sandwich.

those of one β-strand in the adjacent layer (Figure 13a). In an offset orientation, the side chains of a β-strand in one layer interact primarily with those of two β-strands in the adjacent layer. The exposed edge of this orientation can present both a hydrogen-bonding edge and a hydrophobic ledge, with the potential for interaction with additional β-strands (Figure 13b). This structure and its potential for further interaction are reminiscent of the sticky ends in DNA.

Layered β-Sheets in Protein, Amyloid Fibril, and Amyloid-like Fibril Structures. β-Sandwiches are common layered β-sheet structures in proteins. Transthyretin (TTR), for example, features a β-sandwich structure as described above (Figure 3a). The two layers of β-sheets of TTR pack together to form a rotated layered β-sheet structure in which face-to-face interactions involve offset hydrophobic contact (Figure 14).

The HET-s protein aggregates to form amyloid fibrils, like those in prion diseases. Residues 218−289 of HET-s aggregate into fibrils that feature a β-helix structure, as described above (Figure 6c). Figure 15 illustrates that the HET-s β-helix contains offset layered β-sheets and two side-chain packing interfaces in which face-to-face interactions involve hydrophobic contact, interdigitation, and knob−hole interaction.

The Aβ_{1-40} fibrils associated with Alzheimer's disease feature a four-layered β-sandwich in which two layers of β-sheets in a two-layered β-sandwich are layered in an offset fashion (Figure 16a) and face-to-face interactions involve hydrophobic contact and knob−hole interaction (Figures 16b,c). Of particular interest is that glycine, which is not typically thought of as favoring β-sheet formation, plays a special role in the assembly, with residues G_{33}, G_{37}, and G_{38} creating holes for the knob−hole interactions within and between the two-layered β-sandwiches.

The structures of amyloid-like fibrils from amyloidogenic peptide fragments often shed light on amyloid fibril structures and provide useful insights into how amyloid self-assembles into fibrils.[32] The crystallographic structure of GNNQQNY from prion protein Sup35 shows that it self-assembles into an offset layered β-sheet structure in which face-to-face interactions involve interdigitation (Figure 17a).[32a] NMR-based structural models show that the central residues AAAAGAVV of peptide fragment $PrP_{106-126}$ from the human prion protein self-assemble into a rotated layered β-sheet structure in which face-to-face interactions involve interdigitation (Figure 17b).[33] The crystallographic structure of KLVFFA from Aβ shows that it self-assembles into an aligned layered β-sheet structure in which face-to-face interactions involve aligned and offset hydrophobic contact (Figure 17c).[32g]

■ CHEMICAL MODELS OF β-SHEETS

Chemical model systems provide a powerful platform with which to study and control the rich supramolecular chemistry of β-sheets. Our laboratory has developed macrocyclic β-sheet peptides containing artificial turn and template units as chemical models of β-sheet structure and interactions. The macrocyclic β-sheets contain a natural peptide β-strand, turns

dx.doi.org/10.1021/ja3088407 | J. Am. Chem. Soc. 2013, 135, 5477−5492

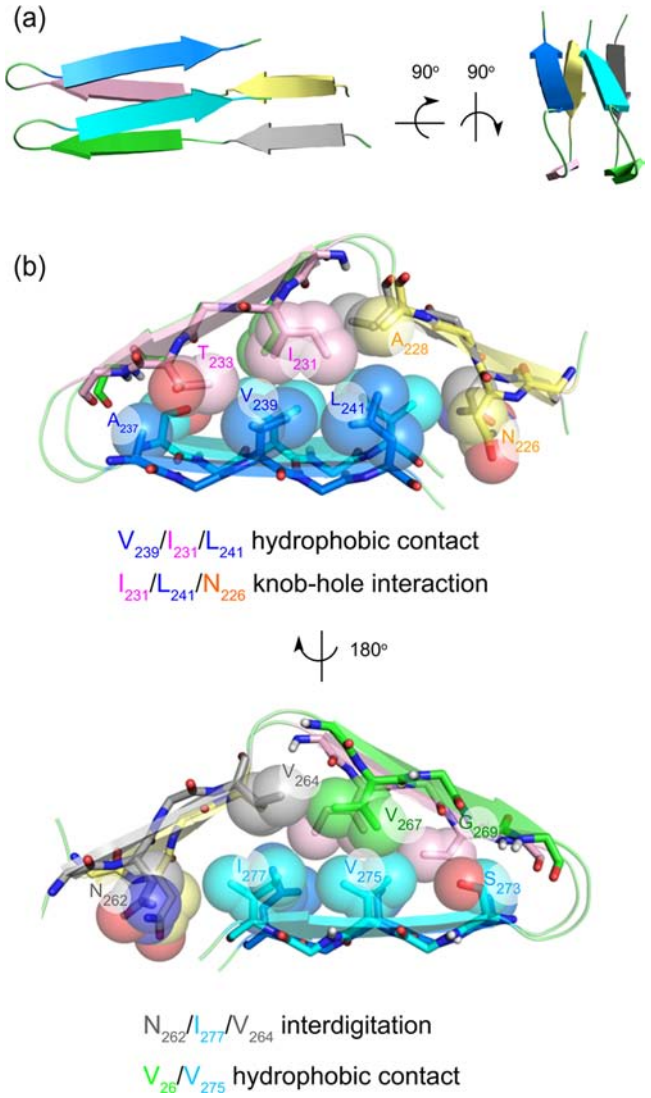

Figure 15. Orientation and face-to-face interactions in the layered β-sheets of the HET-s β-helix (PDB: 2RNM). (a) Offset layered β-sheets of residues 218−289 of HET-s. (b) The i/j and $i/j/i + 2$ hydrophobic contacts, $i/j/i + 2$ interdigitation, and $i - 2/j/i + 2$ knob−hole interaction in residues 218−289 of HET-s.

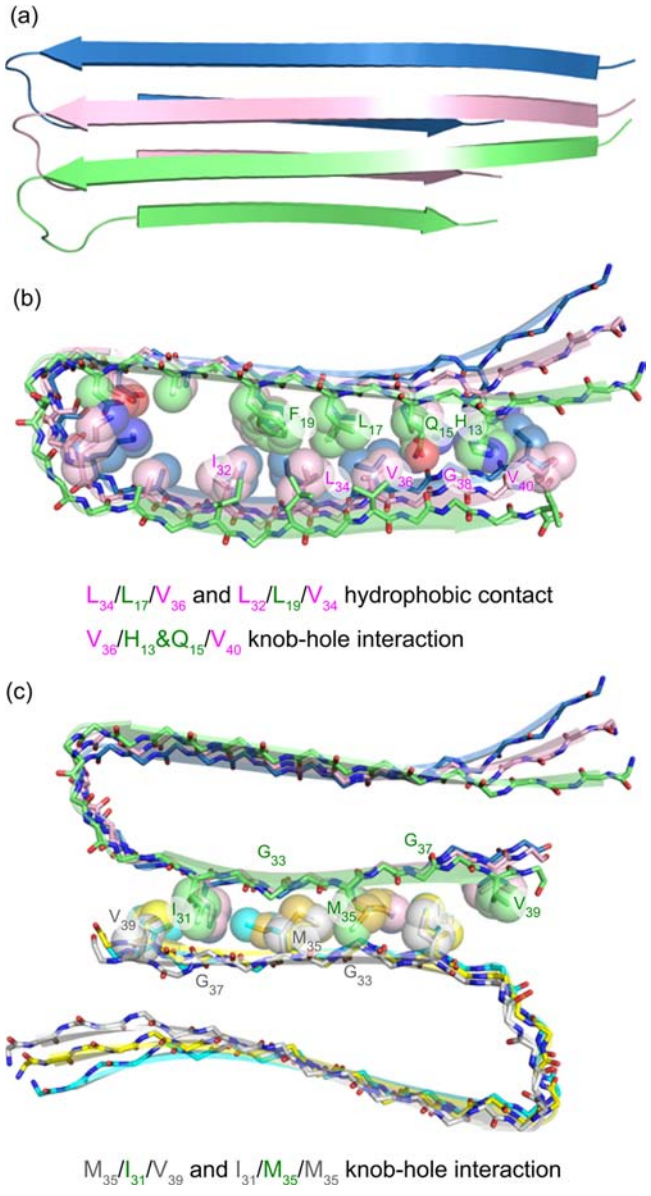

Figure 16. Orientation and face-to-face interactions in the layered β-sheets in Aβ_{1-40} fibrils. (a) Offset layered β-sheets of the Aβ_{1-40} fibrils. (b) The $i/j/i + 2$ hydrophobic contacts and $i - 2/j/i + 2$ knob−hole interaction in the Aβ_{1-40} fibrils. (c) The $i - 2/j/i + 2$ knob−hole interaction in Aβ_{1-40} fibrils.

based on δ-linked ornithine ($^{\delta}$Orn),[9d,e] and templates based on the unnatural amino acid Hao,[9c] which mimics the hydrogen-bonding edge of a tripeptide β-strand while blocking the other edge. Macrocycles **1**−**3** are the three most important classes of macrocyclic β-sheets that we have thus far published (Figure 18).[9j,l,n,o,q−s]

Macrocyclic β-sheet **1** is a 42-membered ring containing a pentapeptide (upper strand, R_1−R_5), two $^{\delta}$Orn turn units (shown in blue), one Hao template (shown in red), and two additional amino acids (R_6 and R_7).[9l,q,r,t] Macrocyclic β-sheet **2** is a 54-membered ring containing a heptapeptide (upper strand, R_1−R_7), two $^{\delta}$Orn turn units, two Hao templates, and one additional amino acid (R_8).[9j,n,o] Macrocyclic β-sheet **3** is a 54-membered ring containing a heptapeptide (upper strand, R_1−R_7), two $^{\delta}$Orn turn units, one Hao template, and four additional amino acids (R_8−R_{11}).[9s]

Macrocyclic β-sheets **1**−**3** exhibit a rich supramolecular chemistry. The penta- and heptapeptide strands of these macrocycles provide one exposed edge that can participate in edge-to-edge hydrogen-bonding interactions. The Hao-containing strands help preorganize the other edge by intramolecular hydrogen bonding, while blocking further hydrogen-bonding interactions. The side chains of the alternate amino acids of the penta- and heptapeptide strands, above and below the hydrogen-bonded backbones, make up the "top" and "bottom" faces of the β-sheet.

Table 1 illustrates some of the macrocyclic β-sheets that have demonstrated edifying supramolecular chemistry in the solid state or in solution. Many of these macrocycles contain penta- and heptapeptides derived from amyloidogenic or other β-sheet peptides and proteins. The pentapeptides of **1a**, **1b**, and **1e** are based on residues 17−21 and 30−34 of Aβ, while those of **1c** and **1d** are based on residues 306−310 of tau. The heptapeptides of **2a** and **2b** are based on protein G variant NuG2.[34] The heptapeptides of **3a** and **3b** are based on residues

dx.doi.org/10.1021/ja3088407 | J. Am. Chem. Soc. 2013, 135, 5477−5492

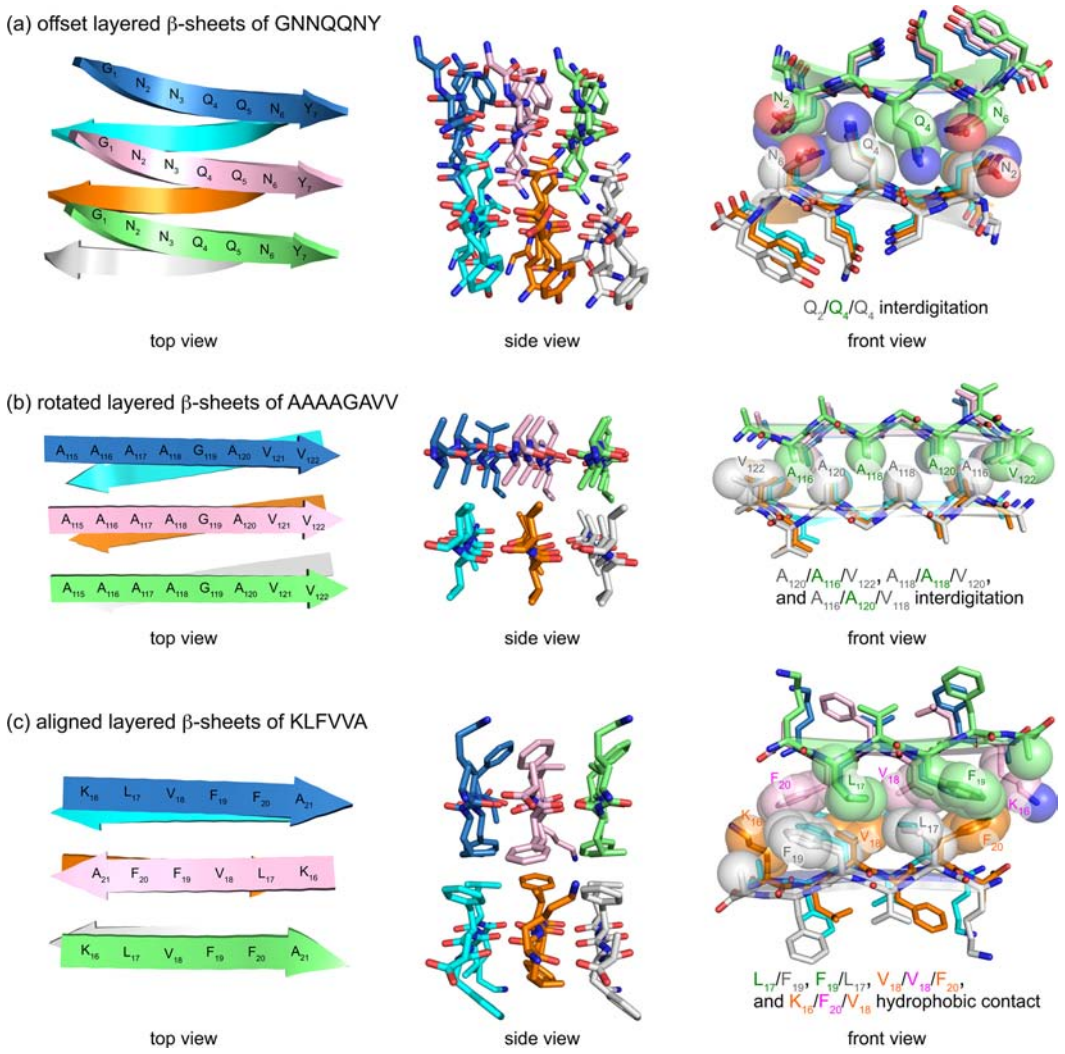

Figure 17. Orientations and face-to-face interactions in the layered β-sheets from amyloidogenic peptide fragments. (a) Crystal structure of GNNQQNY (PDB: 1YJP). (b) NMR-based structural model of AAAAGAVV. (c) Crystal structure of KLVFFA (PDB: 3OW9).

30−36 and 16−22 of Aβ, while that of **3c** is based on residues 63−69 of human β_2-microglobulin (hβ_2M) and that of **3d** is based on human α-synuclein (hαSyn).

Folding of Macrocyclic β-Sheets. The X-ray crystallographic structures of macrocycles **1a**−**1c**, **2b**, and **3a** reveal well-folded β-sheet structures in the solid state.[9q,o,s] The main chains of 42-membered ring macrocycles **1a**−**1c** have six intramolecular hydrogen bonds between the upper and lower strands and adopt similar conformations (Figure 19).[9q] The main chains of 54-membered ring macrocycles **2b** and **3a** have eight intramolecular hydrogen bonds between the upper and lower strands (Figure 20).[9o,s]

The X-ray crystallographic structures of macrocycles **1b**, **1c**, and **3a** exhibit a pronounced twist. This twist can stabilize the folded structure of macrocycle **1** through hydrophobic or van der Waals interactions between residues R_4 and R_6 and the two $^{\delta}$Orn turn units (Figure 21). These interactions can be observed in the X-ray crystallographic structures of macrocycles **1b** and **1c**. ^{1}H NMR spectroscopic studies of macrocycles **1** suggest that bulky and branched residues at the R_4 and R_6 positions also enhance the formation of folded β-sheet structures in aqueous solution.[9l] This twist can also stabilize the folded structure of macrocycle **3** through hydrophobic or van der Waals interactions between residues R_6 and R_{10} and the two $^{\delta}$Orn turn units. The interaction between R_6 and the adjacent $^{\delta}$Orn turn unit is observed in the X-ray crystallographic structure of macrocycle **3a**, while that between R_{10} is supplanted by other crystal packing interactions. These interactions can, in turn, stabilize the twist of the macrocycles.

Dimerization of Macrocyclic β-Sheets through Edge-to-Edge Hydrogen Bonding. Macrocycles **1a**−**1c**, **2b**, and **3a** do not occur as isolated monomers in the solid state but rather dimerize through edge-to-edge hydrogen bonding. All of the macrocycles form dimers in which the two monomers interact to form an antiparallel β-sheet; macrocycle **1a** forms both parallel and antiparallel β-sheet dimers in the same lattice. Figures 22 and 23 illustrate the structures of the six observed dimers with line drawings, and Figures 24 and 25 show the crystal structures.

Of the five antiparallel β-sheet dimers observed, two (**1a** and **2b**) are in register, with all residues aligned, while three (**1b**, **1c**, and **3a**) are out of register, shifted by two residues. The parallel β-sheet dimer of macrocycle **1a** is shifted out of register by one residue, because the topology of the macrocycles prevents the formation of the type of parallel in-register β-sheets that occur in most amyloid fibrils.

dx.doi.org/10.1021/ja3088407 | J. Am. Chem. Soc. 2013, 135, 5477−5492

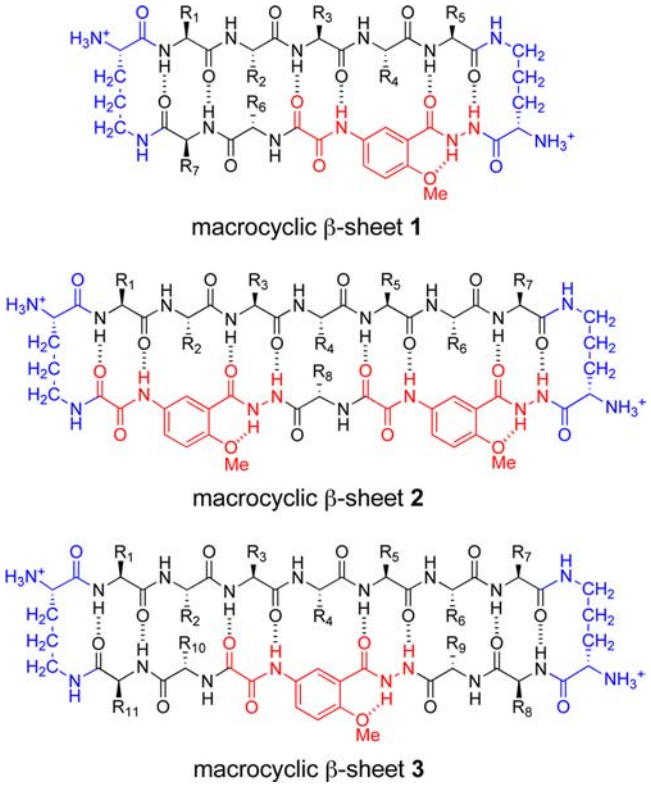

Figure 18. Macrocyclic β-sheets **1**–**3**. The tripeptide mimic Hao is shown in red, and the $^{\delta}$Orn turn units are shown in blue. Intramolecular hydrogen bonds are shown with dashed lines.

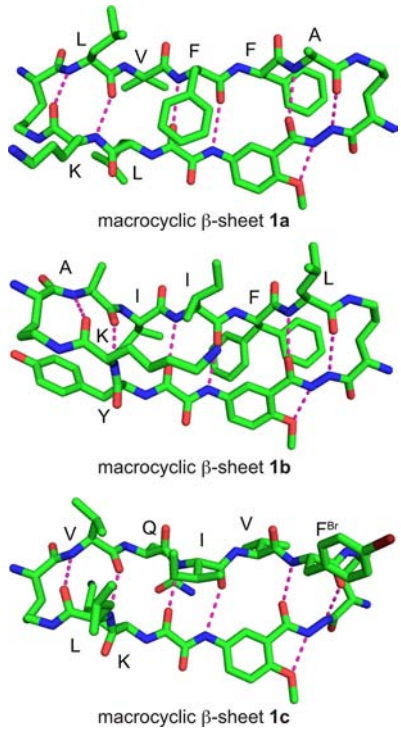

Figure 19. Crystal structures of macrocyclic β-sheets **1a**–**1c** (PDB: 3Q9H, 3Q9J, and 3Q9G). Intramolecular hydrogen bonds are shown with dashed lines. The phenylalanine residue of **1b** exhibits partial occupancy; the two rotameric orientations of the side chain are shown.

All three of the out-of-register antiparallel β-sheet dimers shift by two residues in the same direction—toward the C-terminus. Shifting by two residues, rather than by one or three, is necessary to hydrogen bond; shifts of homodimers of antiparallel β-sheets by an even number of residues is possible; and shifts of homodimers of antiparallel β-sheets by an odd number of residues is not. While shifting toward the C-terminus costs hydrogen bonds, it can provide better hydrophobic or van der Waals interactions. Shifting by two residues brings together the bulky isoleucine and leucine residues in the NHB rings of the **1b** dimer interface and the bulky isoleucine, leucine, and valine residues in the NHB rings of the **3a** dimer interface. The resulting hydrophobic patch helps stabilize the further assembly of each dimer into a tetramer, as described in the following section.

The twist of the antiparallel β-sheets brings together residues in adjacent NHB rings and helps create additional favorable hydrophobic or van der Waals interactions. The β-sheet dimerization interface of macrocycle **3a** illustrates these stabilizing interactions (Figure 26). In addition to the three sets of primary intersheet interactions between the side chains of the valine and isoleucine, leucine and leucine, and isoleucine and valine, there are four sets of secondary intersheet interactions, between the valine and alanine, leucine and isoleucine, isoleucine and leucine, and alanine and valine. These interactions, in turn, stabilize the twist of the β-sheets.

Face-to-Face Interactions of Macrocyclic β-Sheets. The dimers of macrocycles **1a**–**1c**, **2b**, and **3a** pack in the solid

Table 1. Amino acids in macrocycles 1-3[a]

macrocycle	R_1	R_2	R_3	R_4	R_5	R_6	R_7	R_8	R_9	R_{10}	R_{11}
1a (based on Aβ_{17-21})	Leu	Val	Phe	Phe	Ala	Leu	Lys				
1b (based on Aβ_{30-34})	Ala	Ile	Ile	Phe	Leu	Tyr	Lys				
1c (based on Tau$_{306-310}$)	Val	Gln	Ile	Val	Phe^{Br}	Lys	Leu				
1d (based on Tau$_{306-310}$)	Val	Gln	Ile	Val	Tyr	Lys	Leu				
1e (based on Aβ_{30-34})	Ala	Ile	Ile	Gly	Leu	Tyr	Lys				
2a (based on NuG2)	Thr	Ser	Phe	Thr	Tyr	Thr	Ser	Lys			
2b (based on NuG2)	Thr	Tyr	Phe	Thr	Tyr	Phe^{Br}	Ser	Lys			
3a (based on Aβ_{30-36})	Ala	Ile	Ile	Gly	Leu	Met	Val	Lys	Phe	Phe^{Br}	Lys
3b (based on Aβ_{16-22})	Lys	Leu	Val	Phe	Phe	Ala	Glu	Lys	Leu	Ile	Glu
3c (based on hβ_2M$_{63-69}$)	Tyr	Leu	Leu	Tyr	Tyr	Thr	Glu	Lys	Val	Val	Lys
3d (based on hαSyn$_{75-81}$)	Thr	Ala	Val	Ala	Asn	Lys	Thr	Val	Phe	Tyr	Lys

[a]Standard three-letter abbreviations are used, and Phe^{Br} represents *p*-bromophenylalanine, which was incorporated to faciliate X-ray crystallographic analysis.

dx.doi.org/10.1021/ja3088407 | *J. Am. Chem. Soc.* 2013, 135, 5477–5492

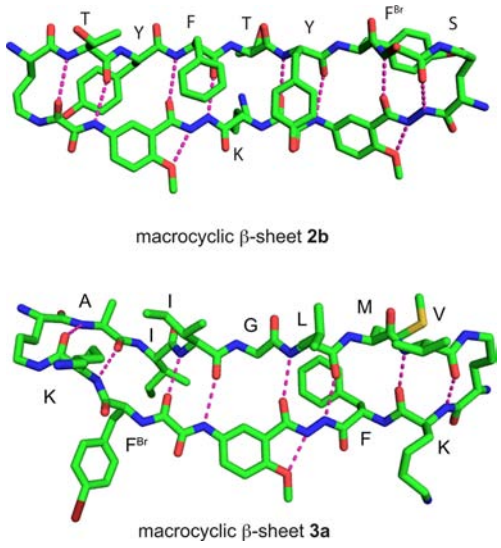

Figure 20. Crystal structures of macrocyclic β-sheets **2b** and **3a** (PDB: 3NI3 and 3T4G). Intramolecular hydrogen bonds are shown with dashed lines.

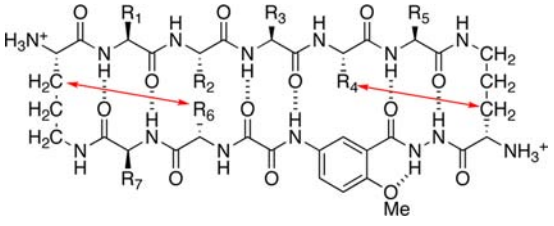

Figure 21. Stabilizing interactions between residues R_4 and R_6 and the two $^{\delta}$Orn turn units in macrocycle **1** facilitated by the natural right-handed twist of the β-sheet (represented with red arrows).

state through face-to-face interactions to form tetramers and related higher-order assemblies. Macrocycle **1c** packs in the lattice as tetramers comprising dimers of dimers that interact through hydrophobic face-to-face interactions (Figure 27). The dimer subunits of the tetramers pack in a symmetrical face-to-face fashion, rather than an unsymmetrical face-to-back fashion. These inner faces present the hydrophobic valine (R_1), isoleucine (R_3), and *p*-bromophenylalanine (R_5) residues of the pentapeptide in the upper strand as well as the hydrophobic leucine (R_7) residue in the lower strand. These residues pack together to make up the hydrophobic core of the tetramer. The layers of the sheets are rotated at nearly right angles with respect to each other, allowing the twisted β-sheets to clasp together and create a tightly packed hydrophobic core. The tetramers are relatively isolated, having little contact with each other, except stacking interactions between the Hao templates.

Macrocycle **1b** also packs in the lattice as tetramers comprising dimers of dimers that interact through hydrophobic face-to-face interactions (Figure 28). The hydrophobic alanine (R_1), isoleucine (R_3), and leucine (R_5) residues of the pentapeptide in the upper strand pack together to make up the hydrophobic core of the tetramer. The tetramers stack loosely on each other through interactions among the phenylalanine groups on the outer faces of the tetramers. Zinc ions, which crystallized with **1b**, coordinate to the $^{\delta}$Orn turn units, and both span and bridge the tetramer units.

Macrocycle **1a** forms stacks of four dimers in the lattice that make up a four-layered β-sandwich structure, with the parallel

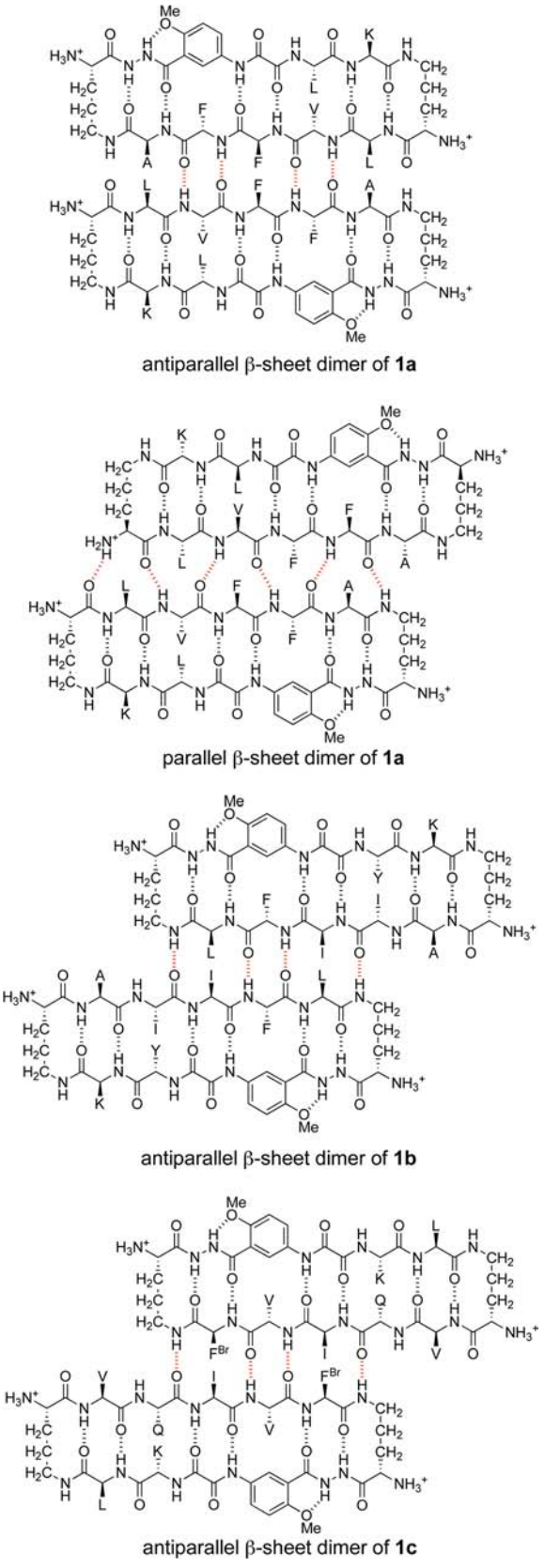

Figure 22. Dimers of macrocyclic β-sheets **1a**–**1c** observed by X-ray crystallography. Intermolecular hydrogen bonds are shown with red dashed lines.

β-sheet dimers as the top and bottom layers of the stack and the antiparallel β-sheet dimers as the middle two layers of the

dx.doi.org/10.1021/ja3088407 | J. Am. Chem. Soc. 2013, 135, 5477–5492

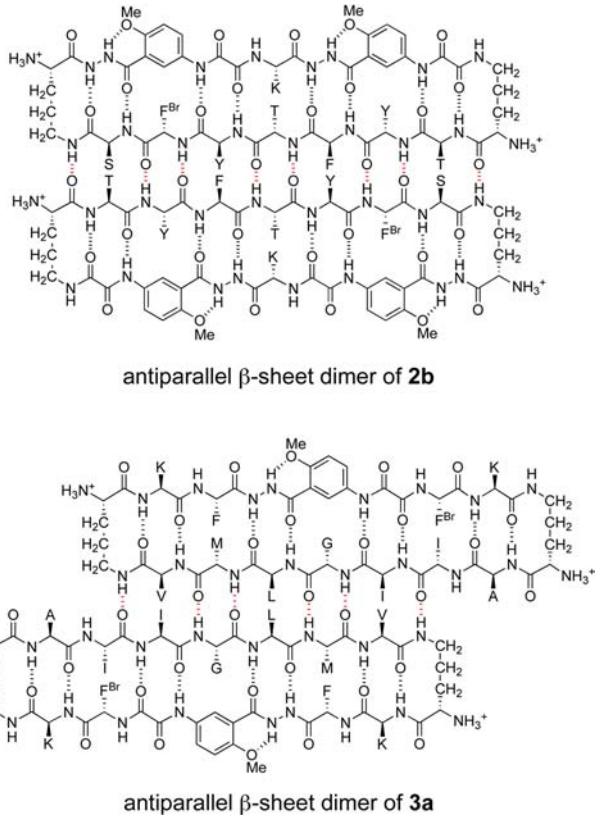

Figure 23. Dimers of macrocyclic β-sheets **2b** and **3a** observed by X-ray crystallography. Intermolecular hydrogen bonds are shown with red dashed lines.

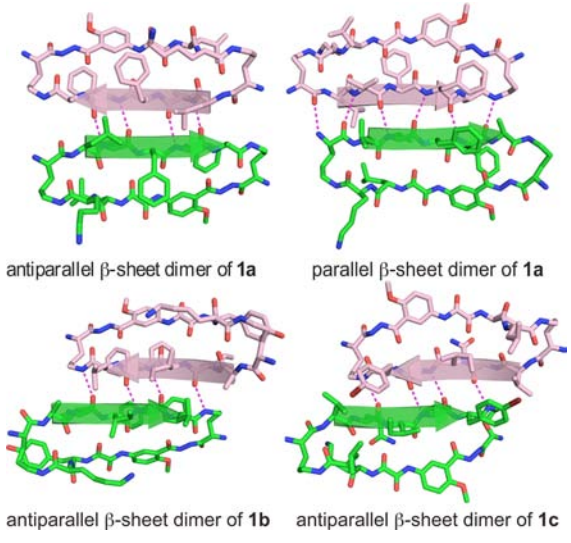

Figure 24. Crystal structures of dimers of macrocyclic β-sheets **1a**−**1c** (PDB: 3Q9H, 3Q9J, and 3Q9G). Intermolecular hydrogen bonds are shown with dashed lines.

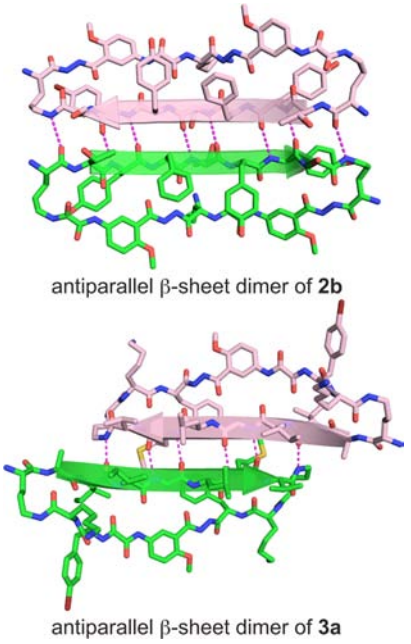

Figure 25. Crystal structures of dimers of macrocyclic β-sheets **2b** and **3a** (PDB: 3NI3 and 3T4G). Intermolecular hydrogen bonds are shown with dashed lines.

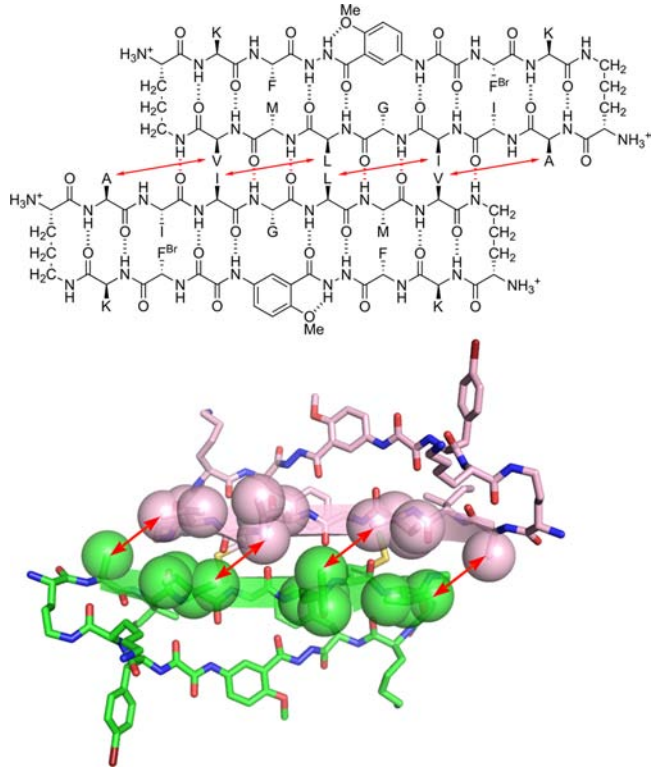

Figure 26. Dimer of macrocyclic β-sheet **3a** showing stabilizing secondary interactions facilitated by the natural right-handed twist of the β-sheet (represented with red arrows).

stack. These stacks may be thought of as encompassing two types of tetramers: a face-to-face tetramer composed of two antiparallel β-sheet dimers (tetramer 1) and an unsymmetrical tetramer composed of an antiparallel β-sheet dimer and a parallel β-sheet dimer (tetramer 2). Figure 29 illustrates these tetramers. Residues R_1−R_5 of the macrocycle are all hydrophobic, making both faces of the pentapeptide hydrophobic and allowing both types of tetramers to have hydrophobic cores.

Macrocycle **3a** also forms stacks of β-sheet dimers that may be thought of as comprising two types of tetramer: a face-to-face tetramer (tetramer 1) and a back-to-back tetramer (tetramer 2). Figure 30 illustrates these tetramers. The

dx.doi.org/10.1021/ja3088407 | J. Am. Chem. Soc. 2013, 135, 5477−5492

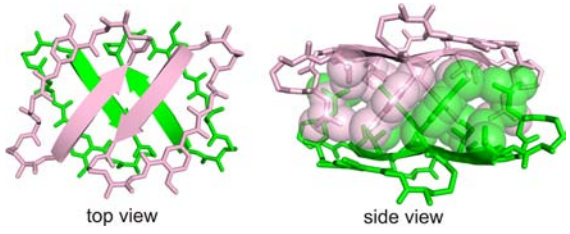

Figure 27. Crystal structure of the tetramer of macrocyclic β-sheet **1c** (PDB: 3Q9G). Top view shows the relative orientations of the macrocycles. Side view shows the hydrophobic core. Selected side chains are omitted for clarity.

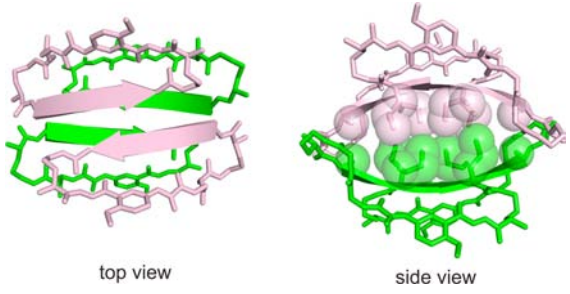

Figure 28. Crystal structure of the tetramer of macrocyclic β-sheet **1b** (PDB: 3Q9J). Top view shows the relative orientations of the macrocycles. Side view shows the hydrophobic core. Zinc ions and selected side chains are omitted for clarity.

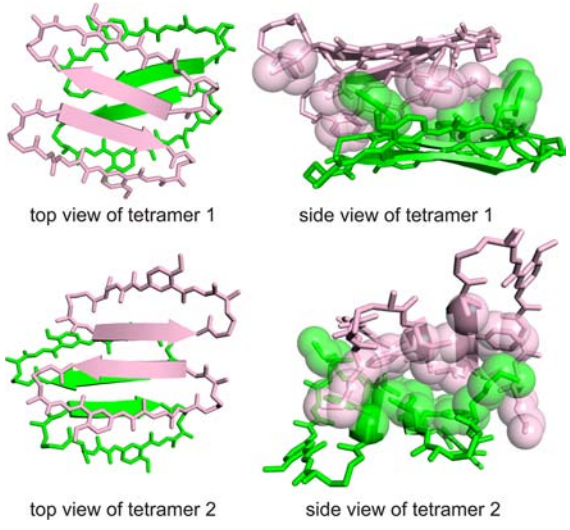

Figure 29. Crystal structure of the tetramers of macrocyclic β-sheet **1a** (PDB: 3Q9H). Top views show the relative orientations of the macrocycles. Side views show the hydrophobic cores. Selected side chains are omitted for clarity.

isoleucine (R_3), leucine (R_5), and valine (R_7) residues of the heptapeptide in the upper strand create the hydrophobic core of the face-to-face tetramer. The methionine (R_6) residue of the heptapeptide in the upper strand and the phenylalanine (R_9) in the lower strand create the hydrophobic core of the back-to-back tetramer. The layers of the sheets of the back-to-back tetramer (tetramer 2) are rotated at nearly right angles with respect to each other and clasp together, like those of the tetramer of macrocycle **1c**. The layers of the face-to-face tetramer (tetramer 1), on the other hand, are aligned and twist in a laminated fashion.

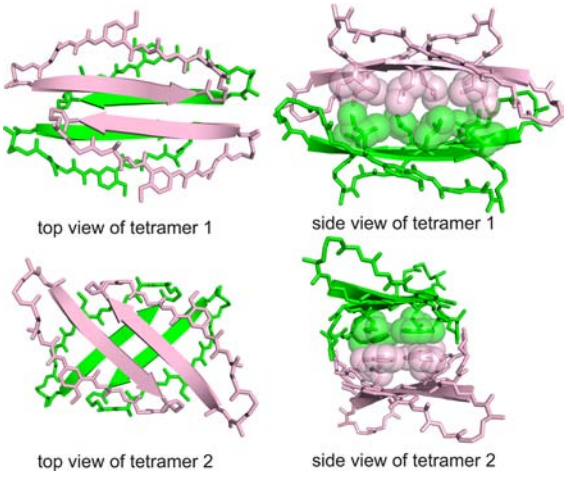

Figure 30. Crystal structures of the tetramers of macrocyclic β-sheet **3a** (PDB: 3T4G). Top views show the relative orientations of the macrocycles. Side views show the hydrophobic cores. Selected side chains are omitted for clarity.

Macrocycle **2b** crystallizes as hexamers comprising trimers of dimers, rather than tetramers comprising dimers of dimers. The hexamer may be thought of as a β-sandwich in which one of the layers has been tilted upward by 60°, and another dimer has been added to create a triangular assembly. In solution, homologue **2a** forms tetramers comprising dimers of dimers, in which the phenylalanine (R_3) and tyrosine (R_5) residues of the heptapeptide in the upper strand pack together to create a hydrophobic core. This tetramer resembles the tetramers formed by macrocycles **1a**–**1c** and **3a**.

The tetramers formed by these macrocyclic β-sheets may shed light on the structures of the oligomers that are central to the toxicity of amyloids in Alzheimer's and other neurodegenerative diseases. In the tetramers, hydrophobic or van der Waals interactions act in conjunction with hydrogen bonding to create recognizable assemblies with common structural themes: folded monomers with β-sheet structures that assemble to hydrogen-bonded dimers that pack face-to-face or back-to-back to form layered structures. All of these features reflect the self-complementarity of these peptides and hence their ability to form oligomers. When the layers of the sheets are substantially rotated with respect to each other, the twist of the β-sheets creates a special additional complementarity in which two corners of the upper sheet clasp two corners of the lower sheet. This clasping together of the rotated twisted β-sheets may help create oligomers with well-packed cores, enhanced stability, and unique biological properties.

Macrocyclic β-Sheets that Inhibit Amyloid Aggregation. Macrocyclic β-sheets containing amyloid-derived peptide sequences can control the aggregation of amyloidogenic peptides and proteins through the same types of supramolecular interactions that occur among β-sheets. The macrocycles are designed to bind to β-sheet intermediates involved in the aggregation process and block further aggregation. Macrocyclic β-sheet **1d** inhibits the aggregation of an amyloidogenic hexapeptide from the protein tau, which aggregates to form neurofibrillary tangles in Alzheimer's disease and certain frontotemporal dementias.[9r] Both edge-to-edge hydrogen bonding and face-to-face hydrophobic interactions are essential to the binding process, and the macrocycle appears to interact with the offset layered β-sheets of the amyloidogenic

dx.doi.org/10.1021/ja3088407 | J. Am. Chem. Soc. 2013, 135, 5477–5492

hexapeptide through hydrogen-bonding interactions with an exposed hydrogen-bonding edge and hydrophobic interactions with a hydrophobic ledge. The inhibition appears to involve two molecules binding cooperatively to the two layers of the aggregating β-sheets.

Macrocyclic β-sheet **3b** inhibits Aβ aggregation and reduces the toxicity of amyloid aggregates.[9s] Macrocyclic β-sheet **3c** inhibits the aggregation of human β_2-microglobulin (hβ_2M), which is associated with dialysis-related amyloidosis.[9s] Macrocyclic β-sheet **3d** inhibits the aggregation of human α-synuclein (hαSyn), which is associated with Parkinson's disease.[9s] Heterodivalent compounds comprising macrocyclic β-sheets **1a** and **1e** connected by a polyethyene-glycol-based linker inhibit Aβ aggregation more strongly than the monovalent components **1a** and **1e** or homodivalent molecules containing two copies of **1a** or **1e** connected by a polyethylene-glycol-based linker.[9t]

CONCLUSION AND OUTLOOK

Our chemical model systems have given us deeper insights into the rich supramolecular chemistry of β-sheets and have helped us better understand the types of supramolecular interactions in protein quaternary structure and in amyloids. A unifying theme that has emerged in both the model systems and natural proteins and amyloids is the confluence of edge-to-edge hydrogen-bonding interactions and face-to-face hydrophobic interactions among β-sheets that result in layered sandwich-like structures. The characteristic right-handed twist of β-sheets can help stabilize edge-to-edge interactions among β-sheets through favorable secondary interactions between hydrophobic side chains in adjacent NHB rings. Complementarity among the faces of the β-sheets is particularly important, through features, such as aligned and offset hydrophobic contacts, interdigitation, and knob−hole interactions. The orientation of layered β-sheets helps maximize the complementarity of the layered structures. Twisted β-sheets can clasp together in rotated layered structures to create compact oligomers with well-packed cores. Offset layered β-sheets with hydrogen-bonding edges over hydrophobic ledges have special potential for further interactions and may be especially important in β-sheet aggregation. By understanding and applying these principles, it may be possible to gain unique insights with which to further control β-sheet interactions in Alzheimer's and other diseases and to ultimately develop therapies.

AUTHOR INFORMATION

Corresponding Author

jsnowick@uci.edu

Notes

The authors declare no competing financial interest.

ACKNOWLEDGMENTS

We thank the National Institutes of Health (1R01GM097562) and NSF (CHE-1112188) for grant support and Drs. Robert Tycko and Simon Sharpe for providing coordinates of models of A$\beta_{1\text{-}40}$ and PrP$_{106\text{-}126}$. We thank Drs. David Eisenberg, Michael Sawaya, Cong Liu, Minglei Zhao for elucidating the crystallographic structures of macrocycles **1a−1c**, **2b**, and **3a** and for insightful analyses and thoughtful discussions of these and other structures.

REFERENCES

(1) (a) Alberts, B.; Johnson, A.; Lewis, J.; Raff, M.; Roberts, K.; Walter, P. *Molecular Biology of the Cell*, 5th ed.; Garland Press: New York, 2007. (b) Branden, C.; Tooze, J. *Introduction to Protein Structure*, 2nd ed.; Garland Press: New York, 1999.

(2) (a) Maitra, S.; Nowick, J. S. In *The Amide Linkage: Structural Significance in Chemistry, Biochemistry, and Materials Science*; Greenberg, A., Breneman, C. M., Liebman, J. F., Eds.; Wiley: New York, 2000; pp 495−518. (b) Remaut, H.; Waksman, G. *Trends Biochem. Sci.* **2006**, *31*, 436−444.

(3) Münch, J.; Rücker, E.; Ständker, L.; Adermann, K.; Goffinet, C.; Schindler, M.; Wildum, S.; Chinnadurai, R.; Rajan, D.; Specht, A.; Giménez-Gallego, G.; Sánchez, P. C.; Fowler, D. M.; Koulov, A.; Kelly, J. W.; Mothes, W.; Grivel, J.-C.; Margolis, L.; Keppler, O. T.; Forssmann, W.-G.; Kirchhoff, F. *Cell* **2007**, *131*, 1059−1071.

(4) (a) Joerger, A. C.; Fersht, A. R. *Annu. Rev. Biochem.* **2008**, *77*, 557−582. (b) Xu, J.; Reumers, J.; Couceiro, J. R.; De Smet, F.; Gallardo, R.; Rudyak, S.; Cornelis, A.; Rozenski, J.; Zwolinska, A.; Marine, J.-C.; Lambrechts, D.; Suh, Y.-A.; Rousseau, F.; Schymkowitz, J. *Nat. Chem. Biol.* **2011**, *7*, 285−295.

(5) (a) Haass, C.; Selkoe, D. J. *Nat. Rev. Mol. Cell Biol.* **2007**, *8*, 101−112. (b) Jakob-Roetne, R.; Jacobsen, H. *Angew. Chem., Int. Ed.* **2009**, *48*, 3030−3059. (c) Jaworski, T.; Dewachter, I.; Seymour, C. M.; Borghgraef, P.; Devijver, H.; Kügler, S.; Van Leuven, F. *Biochim. Biophys. Acta, Mol. Basis Dis.* **2010**, *1802*, 808−818. (d) Karran, E.; Mercken, M.; Strooper, B. D. *Nat. Rev. Drug Discovery.* **2011**, *10*, 698−712.

(6) (a) Prusiner, S. *Science* **1991**, *252*, 1515−1522. (b) Prusiner, S. *Science* **1982**, *216*, 136−144. (c) Prusiner, S. B.; Scott, M. R.; DeArmond, S. J.; Cohen, F. E. *Cell* **1998**, *93*, 337−348.

(7) (a) May, B. C. H.; Govaerts, C.; Prusiner, S. B.; Cohen, F. E. *Trends Biochem. Sci.* **2004**, *29*, 162−165. (b) Chiti, F.; Dobson, C. M. *Annu. Rev. Biochem.* **2006**, *75*, 333−366. (c) Luheshi, L. M.; Crowther, D. C.; Dobson, C. M. *Curr. Opin. Chem. Biol.* **2008**, *12*, 25−31. (d) Eisenberg, D.; Jucker, M. *Cell* **2012**, *148*, 1188−1203.

(8) (a) Sievers, S. A.; Karanicolas, J.; Chang, H. W.; Zhao, A.; Jiang, L.; Zirafi, O.; Stevens, J. T.; Munch, J.; Baker, D.; Eisenberg, D. *Nature* **2011**, *475*, 96−100. (b) Härd, T.; Lendel, C. *J. Mol. Biol.* **2012**, *421*, 441−465.

(9) (a) Nowick, J. S.; Smith, E. M.; Pairish, M. *Chem. Soc. Rev.* **1996**, *25*, 401−415. (b) Nowick, J. S. *Acc. Chem. Res.* **1999**, *32*, 287−296. (c) Nowick, J. S.; Chung, D. M.; Maitra, K.; Maitra, S.; Stigers, K. D.; Sun, Y. *J. Am. Chem. Soc.* **2000**, *122*, 7654−7661. (d) Nowick, J. S.; Lam, K. S.; Khasanova, T. V.; Kemnitzer, W. E.; Maitra, S.; Mee, H. T.; Liu, R. *J. Am. Chem. Soc.* **2002**, *124*, 4972−4973. (e) Nowick, J. S.; Brower, J. O. *J. Am. Chem. Soc.* **2003**, *125*, 876−877. (f) Nowick, J. S.; Chung, D. M. *Angew. Chem., Int. Ed.* **2003**, *42*, 1765−1768. (g) Chung, D. M.; Nowick, J. S. *J. Am. Chem. Soc.* **2004**, *126*, 3062−3063. (h) Chung, D. M.; Dou, Y.; Baldi, P.; Nowick, J. S. *J. Am. Chem. Soc.* **2005**, *127*, 9998−9999. (i) Nowick, J. S. *Org. Biomol. Chem.* **2006**, *4*, 3869−3885. (j) Khakshoor, O.; Demeler, B.; Nowick, J. S. *J. Am. Chem. Soc.* **2007**, *129*, 5558−5569. (k) Levin, S.; Nowick, J. S. *J. Am. Chem. Soc.* **2007**, *129*, 13043−13048. (l) Woods, R. J.; Brower, J. O.; Castellanos, E.; Hashemzadeh, M.; Khakshoor, O.; Russu, W. A.; Nowick, J. S. *J. Am. Chem. Soc.* **2007**, *129*, 2548−2558. (m) Khakshoor, O.; Nowick, J. S. *Curr. Opin. Chem. Biol.* **2008**, *12*, 722−729. (n) Khakshoor, O.; Nowick, J. S. *Org. Lett.* **2009**, *11*, 3000−3003. (o) Khakshoor, O.; Lin, A. J.; Korman, T. P.; Sawaya, M. R.; Tsai, S.-C.; Eisenberg, D.; Nowick, J. S. *J. Am. Chem. Soc.* **2010**, *132*, 11622−11628. (p) Cheng, P.-N.; Nowick, J. S. *J. Org. Chem.* **2011**, *76*, 3166−3173. (q) Liu, C.; Sawaya, M. R.; Cheng, P.-N.; Zheng, J.; Nowick, J. S.; Eisenberg, D. *J. Am. Chem. Soc.* **2011**, *133*, 6736−6744. (r) Zheng, J.; Liu, C.; Sawaya, M. R.; Vadla, B.; Khan, S.; Woods, R. J.; Eisenberg, D.; Goux, W. J.; Nowick, J. S. *J. Am. Chem. Soc.* **2011**, *133*, 3144−3157. (s) Cheng, P.-N.; Liu, L.; Zhao, M.; Eisenberg, D.; Nowick, J. S. *Nat. Chem.* **2012**, *4*, 927−933. (t) Cheng, P.-N.; Spencer, R.; Woods, R. J.; Glabe, C. G.; Nowick, J. S. *J. Am. Chem. Soc.* **2012**, *133*, 14179−14184.

(10) (a) Smith, C. K.; Regan, L. *Science* **1995**, *270*, 980−982. (b) Wouters, M. A.; Curmi, P. M. G. *Proteins: Struct., Funct., Bioinf.*

1995, *22*, 119−131. (c) Smith, C. K.; Regan, L. *Acc. Chem. Res.* **1997**, *30*, 153−161. (d) Cootes, A. P.; Curmi, P. M. G.; Ross, C.; Donnelly, C.; Torda, A. E. *Proteins: Struct., Funct., Genet.* **1998**, *32*, 175−189. (e) Fooks, H. M.; Martin, A. C. R.; Woolfson, D. N.; Sessions, R. B.; Hutchinson, E. G. *J. Mol. Biol.* **2006**, *356*, 32−44.

(11) Dou, Y.; Baisnee, P.-F.; Pollastri, G.; Pecout, Y.; Nowick, J.; Baldi, P. *Bioinformatics* **2004**, *20*, 2767−2777.

(12) (a) Chothia, C. *J. Mol. Biol.* **1973**, *75*, 295−302. (b) Wang, L.; O'Connell, T.; Tropsha, A.; Hermans, J. *J. Mol. Biol.* **1996**, *262*, 283−293. (c) Ho, B. K.; Curmi, P. M. G. *J. Mol. Biol.* **2002**, *317*, 291−308.

(13) (a) Blake, C. C. F.; Geisow, M. J.; Swan, I. D. A.; Rerat, C.; Rerat, B. *J. Mol. Biol.* **1974**, *88*, 1−12. (b) Blake, C. C. F.; Oatley, S. J. *Nature* **1977**, *268*, 115−120. (c) Damas, A. M.; Ribeiro, S.; Lamzin, V. S.; Palha, J. A.; Saraiva, M. J. *Acta Crystallogr., Sect. D: Biol. Crystallogr.* **1996**, *52*, 966−972.

(14) Harris, L. J.; Larson, S. B.; Hasel, K. W.; McPherson, A. *Biochemistry* **1997**, *36*, 1581−1597.

(15) Zanotti, G.; Ottonello, S.; Berni, R.; Monaco, H. L. *J. Mol. Biol.* **1993**, *230*, 613−624.

(16) Clantin, B.; Delattre, A.-S.; Rucktooa, P.; Saint, N.; Méli, A. C.; Locht, C.; Jacob-Dubuisson, F.; Villeret, V. *Science* **2007**, *317*, 957−961.

(17) Laganowsky, A.; Liu, C.; Sawaya, M. R.; Whitelegge, J. P.; Park, J.; Zhao, M.; Pensalfini, A.; Soriaga, A. B.; Landau, M.; Teng, P. K.; Cascio, D.; Glabe, C.; Eisenberg, D. *Science* **2012**, *335*, 1228−1231.

(18) (a) Yoder, M. D; Keen, N. T.; Jurnak, F. *Science* **1993**, *260*, 1503−1507. (b) Yoder, M. D.; Jurnak, F. *FASEB J* **1995**, *9*, 335−342. (c) Scavetta, R. D.; Herron, S. R.; Hotchkiss, A. T.; Kita, N.; Keen, N. T.; Benen, J. A. E.; Kester, H. C. M.; Visser, J.; Jurnak, F. *Plant Cell* **1999**, *11*, 1081−1092.

(19) Kanamaru, S.; Leiman, P. G.; Kostyuchenko, V. A.; Chipman, P. R.; Mesyanzhinov, V. V.; Arisaka, F.; Rossmann, M. G. *Nature* **2002**, *415*, 553−557.

(20) Wasmer, C.; Lange, A.; Van Melckebeke, H.; Siemer, A. B.; Riek, R.; Meier, B. H. *Science* **2008**, *319*, 1523−1526.

(21) Blake, C.; Serpell, L. *Structure* **1996**, *4*, 989−998.

(22) (a) Petkova, A. T.; Yau, W.-M.; Tycko, R. *Biochemistry* **2006**, *45*, 498−512. (b) Finder, V. H.; Glockshuber, R. *Neurodegener. Dis.* **2007**, *4*, 13−27. (c) Fändrich, M.; Schmidt, M.; Grigorieff, N. *Trends Biochem. Sci.* **2011**, *36*, 338−345.

(23) (a) Paravastu, A. K.; Leapman, R. D.; Yau, W.-M.; Tycko, R. *Proc. Natl. Acad. Sci. U.S.A.* **2008**, *105*, 18349−18354. (b) Meinhardt, J.; Sachse, C.; Hortschansky, P.; Grigorieff, N.; Fändrich, M. *J. Mol. Biol.* **2009**, *386*, 869−877. (c) Miller, Y.; Ma, B.; Nussinov, R. *Chem. Rev.* **2010**, *110*, 4820−4838.

(24) Steinbacher, S.; Seckler, R.; Miller, S.; Steipe, B.; Huber, R.; Reinemer, P. *Science* **1994**, *265*, 383−386.

(25) Schumacher, M. A.; Funnell, B. E. *Nature* **2005**, *438*, 516−519.

(26) (a) Monaco, H. L.; Rizzi, M.; Coda, A. *Science* **1995**, *268*, 1039−1041. (b) Prapunpoj, P.; Leelawatwattana, L. *FEBS J.* **2009**, *276*, 5330−5341.

(27) (a) Rafferty, J. B.; Somers, W. S.; Saint-Girons, I.; Phillips, S. E. V. *Nature* **1989**, *341*, 705−710. (b) Somers, W. S.; Phillips, S. E. V. *Nature* **1992**, *359*, 387−393.

(28) (a) Okorokov, A. L.; Orlova, E. V. *Curr. Opin. Struct. Biol.* **2009**, *19*, 197−202. (b) Brosh, R.; Rotter, V. *Nat. Rev. Cancer* **2009**, *9*, 701−713.

(29) Jeffrey, P. D.; Gorina, S.; Pavletich, N. P. *Science* **1995**, *267*, 1498−1502.

(30) Wlodawer, A.; Miller, M.; Jaskolski, M.; Sathyanarayana, B. k.; Baldwin, E.; Weber, I. T.; Selk, L. M.; Clawson, L.; Schneider, J.; Kent, S. B. H. *Science* **1989**, *245*, 616−621.

(31) (a) Crick, F. H. C. *Acta Crystallogr.* **1953**, *6*, 689−697. (b) Hadley, E. B.; Testa, O. D.; Woolfson, D. N.; Gellman, S. H. *Proc. Natl. Acad. Sci. U.S.A.* **2008**, *105*, 530−535.

(32) (a) Nelson, R.; Sawaya, M. R.; Balbirnie, M.; Madsen, A. O.; Riekel, C.; Grothe, R.; Eisenberg, D. *Nature* **2005**, *435*, 773−778. (b) Sambashivan, S.; Liu, Y.; Sawaya, M. R.; Gingery, M.; Eisenberg, D. *Nature* **2005**, *437*, 266−269. (c) Nelson, R.; Eisenberg, D. *Curr. Opin. Struct. Biol.* **2006**, *16*, 260−265. (d) Sawaya, M. R.; Sambashivan, S.; Nelson, R.; Ivanova, M. I.; Sievers, S. A.; Apostol, M. I.; Thompson, M. J.; Balbirnie, M.; Wiltzius, J. J.; McFarlane, H. T.; Madsen, A. O.; Riekel, C.; Eisenberg, D. *Nature* **2007**, *447*, 453−457. (e) Wiltzius, J. J. W.; Sievers, S. A.; Sawaya, M. R.; Cascio, D.; Popov, D.; Riekel, C.; Eisenberg, D. *Protein Sci.* **2008**, *17*, 1467−1474. (f) Ivanova, M. I.; Sievers, S. A.; Sawaya, M. R.; Wall, J. S.; Eisenberg, D. *Proc. Natl. Acad. Sci. U.S.A.* **2009**, *106*, 18990−18995. (g) Colletier, J.-P.; Laganowsky, A.; Landau, M.; Zhao, M.; Soriaga, A. B.; Goldschmidt, L.; Flot, D.; Cascio, D.; Sawaya, M. R.; Eisenberg, D. *Proc. Natl. Acad. Sci. U.S.A.* **2011**, *108*, 16938−16943.

(33) Walsh, P.; Simonetti, K.; Sharpe, S. *Structure* **2009**, *17*, 417−426.

(34) (a) Nauli, S.; Kuhlman, B.; Baker, D. *Nat. Struct. Biol.* **2001**, *8*, 602−605. (b) Nauli, S.; Kuhlman, B.; Le Trong, I.; Stenkamp, R. E.; Teller, D.; Baker, D. *Protein Sci.* **2002**, *11*, 2924−2931.